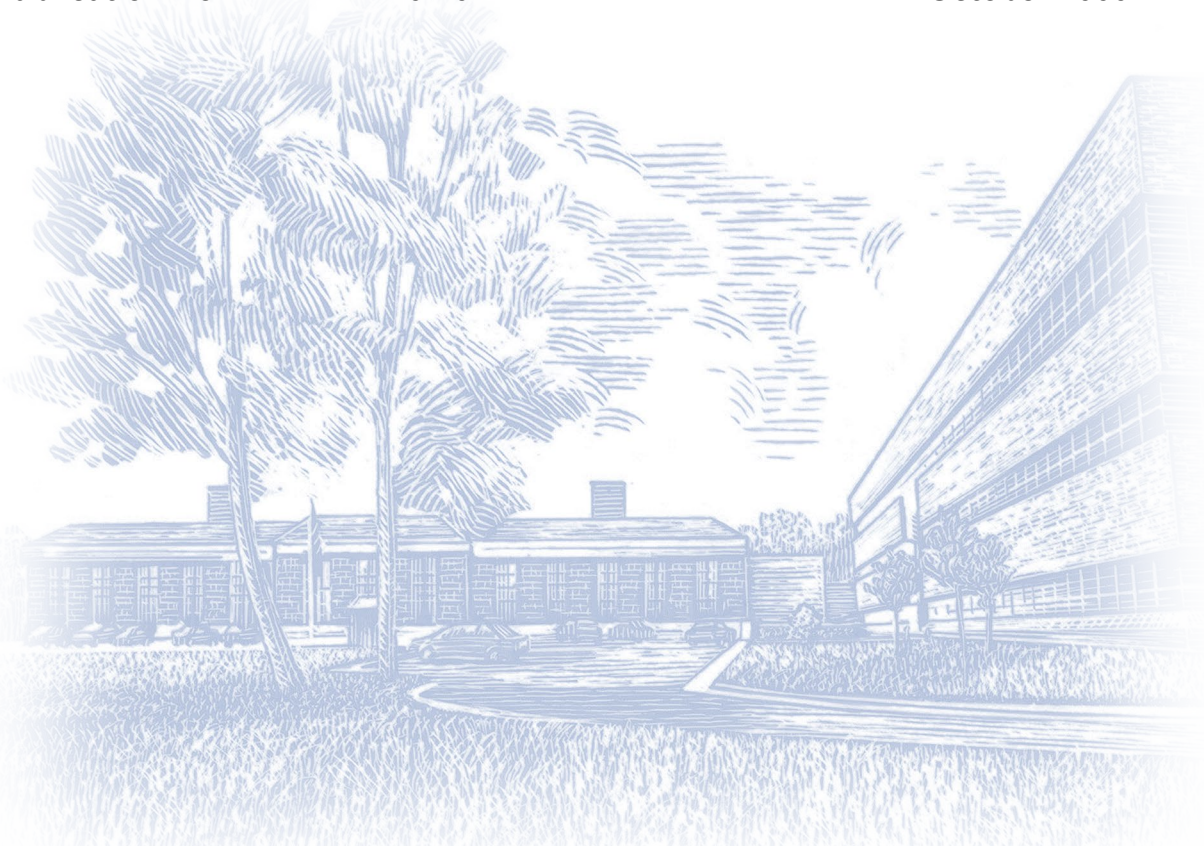


# Modified Asphalt Binders in Mixtures- Topical Report: Permanent Deformation Using A Mixture With Diabase Aggregate

Publication No.: FHWA-RD-02-042

October 2000



The original format of this document was an active HTML page(s). The Federal Highway Administration converted the HTML page(s) into an Adobe® Acrobat® PDF file to preserve and support reuse of the information it contained.

The intellectual content of this PDF is an authentic capture of the original HTML file. Hyperlinks and other functions of the HTML webpage may have been lost, and this version of the content may not fully work with screen reading software.

## Foreword

by

Kevin D. Stuart  
Federal Highway Administration  
Turner-Fairbank Highway Research Center  
6300 Georgetown Pike  
McLean, VA 22101-2296  
TELEPHONE: (202) 493-3073  
FAX: (202) 493-3161

Walaa S. Mogawer, PhD, P.E.  
Civil and Environmental Engineering Department  
University of Massachusetts Dartmouth  
North Dartmouth, MA 02747  
TELEPHONE: (508) 999-8468  
FAX: (508) 999-8964

This report documents the effects of polymer-modified asphalt binders on the rutting resistance of a mixture with diabase aggregate. It is part of a research study titled "Understanding the Performance of Modified Asphalt Binders in Mixtures." This study is partially funded through National Cooperative Highway Research Program (NCHRP) Project 90-07. The objective of NCHRP Project 90-07 is to determine if asphalt binder performance is captured by the Superpave asphalt binder specification developed under the 1987 to 1993 Strategic Highway Research Program, with an emphasis on evaluating the performances of mixtures containing polymer-modified asphalt binders with identical Superpave performance grades, but varied chemistries. Asphalt binder tests developed under NCHRP Project 09-10, titled "Superpave Protocols for Modified Asphalt Binders," are also being evaluated. NCHRP Project 09-10 was completed in February 2001. For the materials tested in this study, good correlations between asphalt binder properties and laboratory mixture rutting resistance were found, which indicate that the current Superpave asphalt binder specification and testing protocols are valid. Additional mixtures will be tested by FHWA to verify these findings. This report will be of interest to highway personnel who use polymer-modified asphalt binders and Superpave.

T. Paul Teng, P.E.  
Director, Office of Infrastructure  
Research and Development

## Notice

This document is disseminated under the sponsorship of the U.S. Department of Transportation in the interest of information exchange. The U.S. Government assumes no liability for the use of the information contained in this document.

The U.S. Government does not endorse products or manufacturers. Trademarks or manufacturers' names appear in this report only because they are considered essential to the objective of the document.

## Quality Assurance Statement

The Federal Highway Administration (FHWA) provides high-quality information to serve Government, industry, and the public in a manner that promotes public understanding. Standards and policies are used to ensure and maximize the quality, objectivity, utility, and integrity of its information. FHWA periodically reviews quality issues and adjusts its programs and processes to ensure continuous quality improvement.



Technical Report Documentation Page

<b>1. Report No.</b> FHWA-RD-02-042	<b>2. Government Accession No.</b>	<b>3 Recipient's Catalog No.</b>
<b>4. Title and Subtitle</b> UNDERSTANDING THE PERFORMANCE OF MODIFIED ASPHALT BINDERS IN MIXTURES: PERMANENT DEFORMATION USING A MIXTURE WITH DIABASE AGGREGATE		<b>5. Report Date</b>
		<b>6. Performing Organization Code</b>
<b>7. Author(s)</b> Kevin D. Stuart and Walaa S. Mogawer		<b>8. Performing Organization Report No.</b>
<b>9. Performing Organization Name and Address</b> Office of Infrastructure Research and Development Federal Highway Administration 6300 Georgetown Pike McLean, VA 22101-2296		<b>10. Work Unit No. (TRAIS)</b>
		<b>11. Contract or Grant No.</b> In-House Report
<b>12. Sponsoring Agency Name and Address</b> Office of Infrastructure Research and Development Federal Highway Administration 6300 Georgetown Pike McLean, Virginia 22101-2296		<b>13. Type of Report and Period Covered</b> Final Report October 2000 - December 2001
		<b>14. Sponsoring Agency Code</b>
<b>15. Supplementary Notes</b> FHWA Contact: Kevin D. Stuart, HRDI-11		
<b>16. Abstract</b> <p>The objective of this study was to determine if the Superpave high-temperature properties of polymer-modified asphalt binders correlate to asphalt mixture rutting resistance. An emphasis was placed on evaluating the rutting resistances of mixtures containing polymer-modified asphalt binders with identical (or close) performance grades, but varied polymer chemistries. This would indicate what types of modification provide properties that are, or are not, correctly captured by the current Superpave asphalt binder specification. Eleven asphalt binders were obtained for this study: two unmodified asphalt binders, an air-blown asphalt binder, and eight polymer-modified asphalt binders. Five binders used in a prior study were also tested.</p> <p>Asphalt binder properties were measured by a dynamic shear rheometer. Mixture rutting resistance was measured by: (1) <math>G^*</math> and <math>G^*/\sin(\delta)</math> from the Superpave Shear Tester (SST) frequency sweep at constant height, (2) cumulative permanent shear strain from the SST repeated shear at constant height (RSCH), (3) French Pavement Rutting Tester (French PRT), and (4) the Hamburg Wheel-Tracking Device. Cumulative permanent shear strain and the French PRT were the primary tests because they were specifically developed to measure rutting resistance.</p> <p>The high-temperature properties of the 11 asphalt binders had a high correlation to mixture rutting resistance as measured by the cumulative permanent shear strains. A weak correlation was found using the French PRT. Both correlations were high when analyzing the data from all 16 asphalt binders. A change in high-temperature PG from 70 to 76 significantly increased rutting resistance based on both tests.</p> <p>The main objective of this study was to determine which asphalt binders provide high-temperature properties that do not agree with mixture rutting resistance. In general, the number of</p>		

discrepancies was low. It is recommended that the asphalt binders be tested using other aggregate types or gradations.

**17. Key Words**

Superpave, asphalt binder specification, permanent deformation, Superpave Shear Tester, SST, French Pavement Rutting Tester, Hamburg Wheel-Tracking Device, polymer-modified asphalt binders.

**18. Distribution Statement**

No restrictions. This document is available to the public through the National Technical Information Service, Springfield, Virginia 22161.

**19. Security Classification (of this report)**

Unclassified

**20. Security Classification (of this page)**

Unclassified

**21. No. of Pages**

57

**22. Price**

Form DOT F 1700.7

Reproduction of completed page authorized



## SI\* (Modern Metric) Conversion Factors

<b>Approximate Conversions to SI Units</b>				
<b>Symbol</b>	<b>When You Know</b>	<b>Multiply By</b>	<b>To Find</b>	<b>Symbol</b>
<b>Length</b>				
<b>in</b>	inches	25.4	millimeters	mm
<b>ft</b>	feet	0.305	meters	m
<b>yd</b>	yards	0.914	meters	m
<b>mi</b>	miles	1.61	kilometers	km
<b>Area</b>				
<b>in<sup>2</sup></b>	square inches	645.2	square millimeters	mm <sup>2</sup>
<b>ft<sup>2</sup></b>	square feet	0.093	square meters	m <sup>2</sup>
<b>yd<sup>2</sup></b>	square yard	0.836	square meters	m <sup>2</sup>
<b>ac</b>	acres	0.405	hectares	ha
<b>mi<sup>2</sup></b>	square miles	2.59	square kilometers	km <sup>2</sup>
<b>Volume</b>				
<b>fl oz</b>	fluid ounces	29.57	milliliters	mL
<b>gal</b>	gallons	3.785	liters	L
<b>ft<sup>3</sup></b>	cubic feet	0.028	cubic meters	m <sup>3</sup>
<b>yd<sup>3</sup></b>	cubic yards	0.765	cubic meters	m <sup>3</sup>
NOTE: volumes greater than 1000 L shall be shown in m <sup>3</sup>				
<b>Mass</b>				
<b>oz</b>	ounces	28.35	grams	g
<b>lb</b>	pounds	0.454	kilograms	kg
<b>T</b>	short tons (2000 lb)	0.907	megagrams (or "metric ton")	Mg (or "t")
<b>Temperature (exact degrees)</b>				
<b>°F</b>	Fahrenheit	5 (F-32)/9 or (F-32)/1.8	Celsius	°C
<b>Illumination</b>				
<b>fc</b>	foot-candles	10.76	lux	lx
<b>fl</b>	foot-Lamberts	3.426	candela/m <sup>2</sup>	cd/m <sup>2</sup>
<b>Force and Pressure or Stress</b>				
<b>lbf</b>	poundforce	4.45	newtons	N

lbf/in <sup>2</sup>	poundforce per square inch	6.89	kilopascals	kPa
---------------------	----------------------------	------	-------------	-----

<b>Approximate Conversions from SI Units</b>				
Symbol	When You Know	Multiply By	To Find	Symbol
<b>Length</b>				
mm	millimeters	0.039	inches	in
m	meters	3.28	feet	ft
m	meters	1.09	yards	yd
km	kilometers	0.621	miles	mi
<b>Area</b>				
mm <sup>2</sup>	square millimeters	0.0016	square inches	in <sup>2</sup>
m <sup>2</sup>	square meters	10.764	square feet	ft <sup>2</sup>
m <sup>2</sup>	square meters	1.195	square yards	yd <sup>2</sup>
ha	hectares	2.47	acres	ac
km <sup>2</sup>	square kilometers	0.386	square miles	mi <sup>2</sup>
<b>Volume</b>				
mL	milliliters	0.034	fluid ounces	fl oz
L	liters	0.264	gallons	gal
m <sup>3</sup>	cubic meters	35.314	cubic feet	ft <sup>3</sup>
m <sup>3</sup>	cubic meters	1.307	cubic yards	yd <sup>3</sup>
<b>Mass</b>				
g	grams	0.035	ounces	oz
kg	kilograms	2.202	pounds	lb
Mg (or "t")	megagrams (or "metric ton")	1.103	short tons (2000 lb)	T
<b>Temperature (exact degrees)</b>				
°C	Celsius	1.8C+32	Fahrenheit	°F
<b>Illumination</b>				
lx	lux	0.0929	foot-candles	fc
cd/m <sup>2</sup>	candela/m <sup>2</sup>	0.2919	foot-Lamberts	fl
<b>Force and Pressure or Stress</b>				
N	newtons	02.225	poundforce	lbf



<b>kPa</b>	kilopascals	0.145	poundforce per square inch	lbf/in <sup>2</sup>
------------	-------------	-------	----------------------------	---------------------

\* SI is the symbol for the International System of Units. Appropriate rounding should be made to comply with Section 4 of ASTM E380. (Revised March 2003)

## Table of Contents

Foreword.....	3
Notice.....	3
Quality Assurance Statement.....	3
Technical Report Documentation Page .....	5
SI* (Modern Metric) Conversion Factors.....	7
List of Figures.....	10
List of Tables .....	11
1. Background.....	13
2. Objective.....	15
3. Materials .....	15
4. Tests .....	16
5. Evaluation Using $G^*$ and $G^*/\sin\delta$ .....	16
6. Cumulative Permanent Shear Strain .....	17
7. French PRT .....	36
8. Hamburg WTD .....	37
9. Evaluation of Data Without Statistical Analysis .....	44
10. Comparison of Mixture Tests .....	45
11. Conclusions.....	45
12. Recommendations.....	46
13. References.....	46
PERSONNEL .....	52

### List of Figures

Figure 1. $G^*$ of new aggregate blend vs. $G^*$ of original aggregate blend.....	15
Figure 2. Aggregate gradation. ....	22
Figure 3. Diagram of SST chamber. ....	24
Figure 4. Superpave Shear Tester. ....	25
Figure 5. $G^*/\sin\delta$ of the asphalt mixture vs. $G^*/\sin\delta$ of the asphalt binder using the 11 asphalt binders.....	27
Figure 6. $G^*/\sin\delta$ of the asphalt mixture vs. $G^*/\sin\delta$ of the asphalt binder using all 16 asphalt binders.....	27
Figure 7. $G^*/\sin\delta$ of the asphalt mixture at 50°C vs. high-temperature PG using the 11 asphalt binders.....	28
Figure 8. $G^*/\sin\delta$ of the asphalt mixture at 50oC vs. high-temperature PG using all 16 asphalt binders.....	28
Figure 9. $G^*/\sin\delta$ of the asphalt mixture at 2.0 Hz vs. $G^*/\sin\delta$ of the asphalt binder at 2.0 rad/s using the 11 asphalt binders.....	29



Figure 10. $G^*/\sin\delta$ of the asphalt mixture at 2.0 Hz vs. $G^*/\sin\delta$ of the asphalt binder at 2.0 rad/s using all 16 asphalt binders.....	29
Figure 11. Cumulative permanent shear strain vs. $G^*/\sin\delta$ of the asphalt binder at 10.0 rad/s using the 11 asphalt binders.....	32
Figure 12. Log cumulative permanent shear strain vs. log $G^*/\sin\delta$ of the asphalt binder at 10.0 rad/s using all 16 asphalt binders.....	32
Figure 13. Cumulative permanent shear strain at 50°C vs. high-temperature PG using the 11 asphalt binders.....	33
Figure 14. Log cumulative permanent shear strain at 50°C vs. log high-temperature PG using all 16 asphalt binders.....	33
Figure 15. Log cumulative permanent shear strain vs. log $G^*/\sin\delta$ of the asphalt binder at 0.125 rad/s using the 11 asphalt binders.....	34
Figure 16. Log cumulative permanent shear strain vs. log $G^*/\sin\delta$ of the asphalt binder at 0.125 rad/s using all 16 asphalt binders.....	35
Figure 17. French Pavement Rutting Tester.....	38
Figure 18. French PRT wheel and slab.....	38
Figure 19. French PRT rut depth vs. $G^*/\sin\delta$ of the asphalt binder at 0.9 rad/s using the 11 asphalt binders.....	40
Figure 20. Log French PRT rut depth vs. log $G^*/\sin\delta$ of the asphalt binder at 0.9 rad/s using the 11 asphalt binders.....	41
Figure 21. French PRT rut depth vs. $G^*/\sin\delta$ of the asphalt binder at 0.9 rad/s using all asphalt binders.....	41
Figure 22. Log French PRT rut depth vs. log $G^*/\sin\delta$ of the asphalt binder at 0.9 rad/s using all asphalt binders.....	42
Figure 23. French PRT rut depth at 70°C vs. high-temperature PG using the 11 asphalt binders.....	42
Figure 24. French PRT rut depth at 70°C vs. high-temperature PG using all asphalt binders.....	43
Figure 25. Hamburg Wheel-Tracking Device without water.....	43
Figure 26. Rut depth vs. wheel passes from the Hamburg WTD at 58°C.....	44
Figure 27. RSCH cumulative permanent shear strain at 50°C vs. French PRT rut depth at 70°C for the 11 mixtures.....	50
Figure 28. Log RSCH cumulative permanent shear strain at 50°C vs. log French PRT rut depth at 70°C for all mixtures.....	51
Figure 29. Log RSCH cumulative permanent shear strain vs. log FSCH $G^*/\sin\delta$ for all mixtures.....	52

## List of Tables

Approximate Conversions to SI Units.....	7
Approximate Conversions from SI Units.....	8
Table 1. Comparison of SST properties provided by the original and new aggregate blends.....	14
Table 2. Descriptions of the asphalt binders.....	18
Table 3. Performance grade (PG) for each asphalt binder.....	19
Table 4. Aggregate properties for the diabase.....	21
Table 5. Volumetric properties of the mixture.....	22

Table 6. $G^*/\sin\delta$ 's of all binders and mixtures with the materials listed from the highest to lowest mixture $G^*/\sin\delta$ . .....	23
Table 7. $G^*/\sin\delta$ 's of the 11 binders and mixtures with the materials listed from the highest to lowest mixture $G^*/\sin\delta$ . .....	25
Table 8. Replicate data for $G^*/\sin\delta$ at 50°C. ....	26
Table 9. $G^*/\sin\delta$ 's of the asphalt binders vs. cumulative permanent shear strain.....	30
Table 10. Statistical rankings for the 11 asphalt mixtures based on cumulative permanent shear strain.....	31
Table 11. Replicate data for the cumulative permanent shear strains.....	31
Table 12. $G^*/\sin\delta$ 's of the asphalt binders at 10.0, 2.0, and 0.125 rad/s with the asphalt binders listed from highest to lowest $G^*/\sin\delta$ using 0.125 rad/s. ....	34
Table 13. $G^*/\sin\delta$ 's of the asphalt binders vs. the French PRT with the materials listed from the lowest to highest rut depth at 6,000 wheel passes. ....	39
Table 14. Replicate data for the French PRT.....	40
Table 15. $G^*/\sin\delta$ 's of the binders vs. the creep slopes from the Hamburg WTD with the materials listed from highest to lowest slope (highest to lowest resistance to rutting).....	47
Table 16. Replicate data for the Hamburg WTD.....	48
Table 17. Rankings by test type with the material having the most resistance to rutting listed at the top.....	48
Table 18. Numerical rankings by test type where No. 1 has the most resistance to rutting according to the test and No. 11 has the least resistance to rutting. ....	49
Table 19. Coefficients of determination, $r^2$ , using the data from the 11 mixtures.....	49
Table 20. Coefficients of determination, $r^2$ , using the data from all mixtures.....	50

## 1. Background

Pavement and laboratory tests performed on five surface course mixtures during the Federal Highway Administration's (FHWA) 1993 to 2001 Superpave Validation Study provided a good correlation between the rut depth in the asphalt pavement layer at 58°C and several laboratory mixture properties, including: (1) dynamic shear modulus,  $G^*$ , at 40°C, (2) dissipated energy in the form of  $G^*/\sin\delta$  at 40°C, (3) cumulative permanent shear strain at 40°C, (4) rut depths from the French Pavement Rutting Tester (French PRT) at 60°C, and (5) the creep slopes from the Hamburg Wheel-Tracking Device (Hamburg WTD) at 50°C.<sup>(1)</sup> The aggregate gradation and mixture volumetric properties were the same in all five mixtures; only the performance grade (PG) and type of asphalt binder (polymer modified vs. unmodified) were varied. The five asphalt binders were AC-5, AC-10, AC-20, Novophalt™, and Styrelf™-D, having PG's of 58-34, 58-28, 64-22, 76-22, and 82-22, respectively.

$G^*$  and  $G^*/\sin\delta$  at 40°C were measured using Frequency Sweep at Constant Height (FSCH). Cumulative permanent shear strain at 40°C was measured using Repeated Shear at Constant Height (RSCH). These tests were performed in accordance with American Association of State Highway and Transportation Officials (AASHTO) TP7-94, "Method for Determining the Permanent Deformation and Fatigue Cracking Characteristics of Hot-Mix Asphalt (HMA) Using the Simple Shear Test (SST) Device."<sup>(2)</sup> The SST subjects a cylindrical specimen to simple shear. The acronym SST originally stood for Simple Shear Test, but it now also stands for Superpave Shear Tester. Shear properties were also measured at 58°C, but some of the data were highly variable and could not be used. The FHWA's Accelerated Loading Facility (ALF) was used to test the pavements for rutting. One relationship found during the study was:

$$RD = 1.25 + 0.00144 (\text{CPSS}) \quad r^2 = 0.94 \quad (1)$$

where:

RD = Rut depth in the asphalt pavement layer at 58°C, mm.

CPSS = Cumulative permanent shear strain at 5,000 cycles and 40°C  $\mu\text{m}/\text{m}$ .

The relationship between pavement rut depth and each laboratory mixture test was determined so that mixture properties provided by other asphalt binders could be used to predict their relative ALF pavement rutting performances. Testing additional asphalt binders, mainly polymer-modified asphalt binders, is the subject of the study documented in this report. However, two changes to the mixture were made:

- The original aggregate blend consisted of 61-percent No. 68 diabase, 30-percent No. 10 diabase, 8-percent natural sand, and 1-percent hydrated lime. The amount of No. 68 aggregate was deficient so a new stockpile of aggregate was obtained. This was the only aggregate that needed to be replenished. The percent flat and elongated particles using a 3-to-1 length-to-thickness ratio were 16 percent for the new stockpile vs. 22 percent for the original stockpile. This was the only difference in the properties of the aggregates that was found. The percent flat and elongated particles for both stockpiles using a 5-to-1 length-to-thickness ratio were below 1.0 percent. Both stockpiles had average L.A. Abrasions, specific gravities, and percent water absorptions that were within the precision of the test.
- The hydrated lime in the new mixture was replaced with diabase fines because it was thought that the hydrated lime might interact with some of the polymer-modified asphalt binders to be tested in the new study. The effect of the asphalt binders on moisture susceptibility was also to be determined using no antistripping additive.

The asphalt binder content, volumetric properties, maximum specific gravity, percent natural sand, and the aggregate gradation, including the gradation of the material passing the 75- $\mu\text{m}$  sieve, were not changed.

Mixtures with the five asphalt binders were tested by the SST using both the original and new aggregate blends. Table 1 and figure 1 show that the  $G^*$ 's for each mixture at 40°C and the ALF-associated loading frequency of 2.0 Hz were not the same. A linear regression showed that the two sets of  $G^*$ 's correlated to each other. The  $r^2$  was 0.91. Frequencies ranging from 1.0 to 10.0 Hz provided similar differences in  $G^*$ . Even though the data correlated to each other, the changes in  $G^*$  meant that the relationships between ALF pavement rut depth and the various laboratory mixture properties, such as equation 1, were not valid. Because of this, it became more important to use a temperature closer to the PG's of the polymer-modified asphalt binders than to maintain a temperature of 40°C. The test temperature for the SST tests was increased to 50°C. This was thought to be the highest temperature that would provide repeatable data. Table 1 shows that there were discrepancies for the cumulative permanent shear strains where the strains at both 40 and 58°C were obtained in the Superpave Validation Study. The  $r^2$  between the original strains at 40°C and the new strains at 50°C was 0.89.

The only method that could be used to relate the laboratory mixture properties to ALF pavement rutting performance was to develop new relationships using the new laboratory mixture properties. The applicability of this methodology is questionable. It assumes that the new set of mixture data provides the same pavement rutting performances as the original set of data. Because this should not be true, the predicted pavement rut depths should not be correct. Therefore, it must be assumed that the relative differences in the predicted rut depths are valid. If the new and original mixture properties provided by the five asphalt binders did not correlate to each other, this assumption would not be true.

**Table 1. Comparison of SST properties provided by the original and new aggregate blends.**

Asphalt Binder or Mixture	High-Temp. PG After RTFO Aging	FSCH $G^*$ at 2.0 Hz (MPa)		RSCH Cumulative Permanent Shear Strain at 5,000 Cycles ( $\mu\text{m}/\text{m}$ )		
		Original Blend at 40°C	New Blend at 40°C	Original Blend at 40°C	New Blend at 50°C	Original Blend at 58°C
Novophalt	77	236	104	1 830	14 100	ND <sup>1</sup>
Styrelf	88	150	90	3 480	10 500	ND
AC-20	70	103	53	14 820	36 300	34 200
AC-10	65	60	28	17 040	61 300	31 800
AC-5	59	34	16	22 200	85 500	ND

<sup>1</sup>ND = No data.

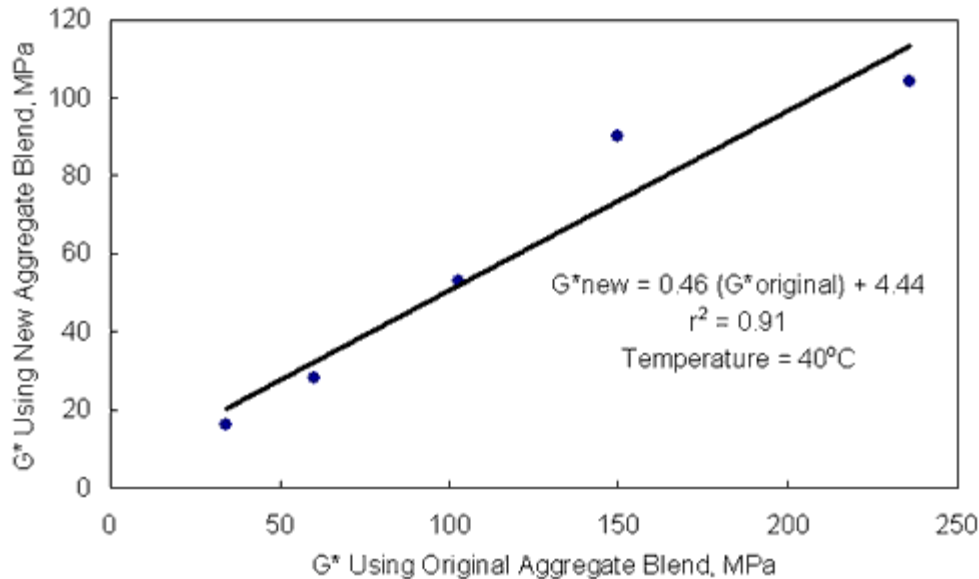


**Figure 1. G\* of new aggregate blend vs. G\* of original aggregate blend.**

## 2. Objective

The objective of this study was to determine if the Superpave high-temperature rheological properties of polymer-modified asphalt binders correlate to asphalt mixture rutting resistance. The emphasis of this study was on evaluating the rutting resistances of mixtures containing polymer-modified asphalt binders with identical high-temperature PG's, but varied chemistries. This would indicate what types of modification provide properties that are, or are not, correctly captured by the current Superpave asphalt binder specification.

## 3. Materials

Eleven asphalt binders were obtained for this study. They consisted of eight polymer-modified asphalt binders: (1) styrene-butadiene-styrene [SBS] Linear, (2) SBS Linear Grafted, (3) SBS Radial Grafted, (4) ethylene vinyl acetate [EVA], (5) EVA Grafted, (6) Elvaloy, (7) ethylene styrene interpolymer [ESI], and (8) chemically modified crumb rubber asphalt [CMCRA]. As shown by this list, the asphalt binders include elastomeric and plastomeric modifiers, some with the same chemistry, but different geometry (linear vs. radial geometries, and grafted vs. ungrafted geometries). The term "grafted" includes any mode of chemically reacting a polymer with an asphalt binder, for example, vulcanization. There were three control asphalts: (1) air-blown, (2) unmodified PG 70-22, and (3) an unmodified PG 64-28. The target PG for the polymer-modified asphalt binders was PG 73-28. Descriptions and rheological properties of the asphalt binders are given in tables 2 and 3. Although identical PG's were desirable, the high-temperature PG's of the polymer-modified asphalt binders ranged from 71 to 77 after rolling thin-film oven (RTFO) aging. The unmodified PG 52-28 asphalt binder was not included in the study. The suppliers of the polymer-modified asphalt binders were allowed to modify this asphalt binder, the unmodified PG 64-28 asphalt binder, or a blend of both asphalts. The five asphalt binders used in the Superpave Validation Study were included, which meant that the total number of asphalt binders was 16.<sup>(1)</sup>

Table 4 shows that the aggregate consisted of 91-percent crushed diabase and 8-percent quartzite natural sand. As previously indicated, the 1-percent hydrated lime was replaced with diabase dust. The aggregate gradation is shown in figure 2.

Mixture properties are given in table 5. The asphalt binder content was 4.85 percent by total mass of the mixture. Additional information on the asphalt binders, aggregates, and the mixtures are given elsewhere.<sup>(1,3)</sup>

## 4. Tests

Asphalt binder properties were measured by a dynamic shear rheometer (DSR) after RTFO aging.<sup>(4)</sup> Mixture rutting resistance was measured by: (1)  $G^*$  and  $G^*/\sin\delta$  using SST FSCH, (2) cumulative permanent shear strain after 5,000 cycles of repeated loading using SST RSCH, (3) rut depths from the French PRT at 6,000 wheel passes, and (4) creep slopes from the Hamburg WTD. The cumulative permanent shear strains from RSCH and the rut depths from the French PRT were considered the primary tests because they were specifically developed to measure rutting resistance. All mixtures were subjected to 2 h of short-term oven aging (STOA) at 135°C.<sup>(1-2)</sup> All specimens were tested approximately 48 h after compaction.

## 5. Evaluation Using $G^*$ and $G^*/\sin\delta$

$G^*$  and the phase angle,  $\delta$ , of each mixture were measured by FSCH at 7.0-percent air voids and 50°C. The total loading time was 0.1 s, which is 10.0 Hz. The data for the 16 mixtures at 10.0 Hz are given in table 6. The SST is shown in figures 3 and 4.

$G^*/\sin\delta$  is often a better indicator of rutting resistance for mixtures containing polymer-modified asphalt binders than  $G^*$ . When  $G^*$  is used to measure rutting resistance, it must be assumed that all mixtures have the same amount of recovered elastic strain after unloading. When this assumption is true, the change in  $G^*$  is proportional to the change in the unrecovered, permanent strain. Thus, mixtures with lower permanent strains have higher  $G^*$ 's. This assumption is not needed when evaluating  $G^*/\sin\delta$  because it is inversely proportional to dissipated energy, or damage. At high temperatures, the susceptibility to rutting should decrease as  $G^*/\sin\delta$  increases. Table 6 shows that  $G^*/\sin\delta$  and  $G^*$  ranked the mixtures similarly. A linear regression provided an  $r^2$  of 0.98. The error of using  $G^*$  to evaluate the mixtures instead of  $G^*/\sin\delta$  is small for this set of data. The largest change in ranking is for the mixture with the PG 70-22 asphalt binder. This mixture has the second highest  $G^*$  (78.9 MPa), but the fifth highest  $G^*/\sin\delta$  (83.9 MPa).

An analysis of variance and Fisher's least squares difference (LSD) were used to rank the 11 mixtures at a 5-percent level of significance. The capital letters in table 7 are the statistical rankings. All mixtures with the same letter have averages that are not significantly different from one another. They are in the same group. All groups are designated by a single letter. However, the groups can overlap. An average with more than one letter indicates that it falls into more than one group. For example, if an average has the designation "A B", it falls into two groups, both A and B. The mixtures from the Superpave Validation Study were not included in the ranking because the main objective of this study was to evaluate the performances of mixtures with modified asphalt binders having similar PG's.

Table 7 shows that many of the 11 mixtures had significantly different  $G^*/\sin\delta$ 's, especially at 2.0 Hz (the use of this frequency is discussed below). The reason for this, as shown by table 8, is that the variability of  $G^*/\sin\delta$  is low. Most coefficients of variation are less than 10 percent. The rankings in table 7 show that grafting did not significantly improve the properties of EVA, and its effect on SBS was marginal.

The correlation between the  $G^*/\sin\delta$ 's of the 11 asphalt binders and the 11 asphalt mixtures, using the standard frequencies of 10.0 Hz and 10.0 rad/s, was poor. The  $r^2$  was 0.50. The  $r^2$  using all 16 materials was 0.72. These relationships are shown in figures 5 and 6, respectively. A log-log transformation increased the  $r^2$  for the 16 materials to 0.79. The relationship in figure 6 indicates that there is a trend of



increasing mixture  $G^*/\sin\delta$  with an increasing binder  $G^*/\sin\delta$ . The regression line should go through the zero-zero origin, but it does not. This indicates that the relationship must be curvilinear.

There was no correlation between the  $G^*/\sin\delta$ 's of the mixtures at 10.0 Hz and continuous high-temperature PG. The  $r^2$  was 0.14. The correlation using all 16 materials was poor. The  $r^2$  was 0.59. These relationships are shown in figures 7 and 8, respectively. Figure 8 does show a trend of increasing mixture  $G^*/\sin\delta$  with increasing high-temperature PG. Poorer correlations could be expected using the high-temperature PG's compared to the  $G^*/\sin\delta$ 's of the asphalt binders at 50°C because the mixtures were tested at 50°C.

The  $G^*/\sin\delta$ 's of the materials were also correlated using 2.0 Hz and 2.0 rad/s because these frequencies are associated with slow-moving traffic. The data are included in table 7. Figures 9 and 10 show that good correlations were obtained. The  $r^2$  was 0.81 for the 11 materials and 0.85 for the 16 materials. As expected, the  $r^2$ 's between the high-temperature PG's and the  $G^*/\sin\delta$ 's of the mixtures at 2.0 Hz and 50°C were not as high. The  $r^2$  was 0.35 for the 11 materials and 0.67 for the 16 materials.

## 6. Cumulative Permanent Shear Strain

Cumulative permanent shear strain was measured at 7.0-percent air voids, 50°C, and 5,000 cycles. The applied shear stress was  $69 \pm 5$  kPa. The loading time was 0.1 s and the rest time was 0.6 s. Three replicate specimens were tested per mixture. Cumulative permanent shear strain is generally a better measure of rutting resistance compared to  $G^*$  and  $G^*/\sin\delta$  because it accounts for changes in the amount of damage from cycle to cycle. Lower cumulative permanent shear strains indicate more resistance to rutting.

The average data for all asphalt binders and mixtures are given in table 9. Rankings for the 11 asphalt mixtures are given in table 10. CMCRA fell into three groups: A, B, and C. Six of the 11 mixtures fell into group C. Six mixtures also fell into group D. This means that even though some of the mixtures had significantly different cumulative permanent shear strains, the range in the strains is relatively low compared to the variability of the strains from replicate specimen to replicate specimen. Table 10 also shows that grafting did not improve the rutting resistance of EVA, and its effect on SBS was not significant.

The replicate strains are given in table 11. The coefficients of variation range from 8.2 to 24.1 percent. Coefficients around 20 percent and lower are generally desirable for asphalt mixture tests. The data indicate that studies on the SST should be done to determine if testing four or five replicate specimens decreases the range in the coefficient of variation.

Figure 11 shows that there was no correlation between the cumulative permanent shear strains and the  $G^*/\sin\delta$ 's of the asphalt binders at 50°C and 10.0 rad/s. The  $r^2$  was 0.08. The  $r^2$  using the data from all 16 materials was 0.43, which is also poor. A log-log transformation increased the  $r^2$  to 0.68. As shown by figure 12, the log-log relationship provided a trend of decreasing cumulative permanent shear strain with increasing  $G^*/\sin\delta$ .

The high-temperature PG's provided relationships as good or better than those provided by  $G^*/\sin\delta$  at 50°C, even though the PG's were 17 to 27°C higher than the SST test temperature of 50°C. The  $r^2$  was 0.68 for the 11 materials. The data are shown in figure 13. However, the data for the PG 64-28 materials might have inflated the  $r^2$ . Without this data point, the  $r^2$  was only 0.39.

The  $r^2$  between high-temperature PG and cumulative permanent shear strain for all 16 materials was 0.69 using no transformation and 0.76 using a log-log transformation. The latter relationship, given in figure 14, shows that there is a trend of decreasing cumulative permanent shear strain with increasing  $G^*/\sin\delta$ . Based on this relationship, an increase of one high-temperature PG, from 70 to 76, would decrease the cumulative permanent shear strain from 28 750 to 18 100  $\mu\text{m}/\text{m}$  at 50°C, which is a 37-percent reduction.

The time-temperature superposition principle indicates that data taken at high temperatures and short loading times can be used to calculate data at lower temperatures and longer loading times. This principle and the higher  $r^2$ 's provided by the high-temperature PG's compared to  $G^*/\sin\delta$  at 50°C and 10 rad/s indicate that  $G^*/\sin\delta$ 's at a frequency lower than 10.0 rad/s should correlate better with cumulative permanent shear strain.  $G^*/\sin\delta$ 's for the 16 materials at 50°C and 10.0, 2.0, and 0.125 rad/s are given in table 12. The latter two frequencies were chosen because the  $G^*/\sin\delta$ 's of the five asphalt binders used in the Superpave Validation Study were measured at these frequencies. For the 11 materials, frequencies of 10.0, 2.0, and 0.125 rad/s provided  $r^2$ 's of 0.06, 0.55, and 0.89, respectively, using log-log transformations. For the 16 materials, frequencies of 10.0, 2.0, and 0.125 rad/s provided  $r^2$ 's of 0.68, 0.83, and 0.93, respectively, using log-log transformations. The relationships using 0.125 rad/s are shown in figures 15 and 16. To avoid having a negative log  $G^*/\sin\delta$ , the unit for  $G^*/\sin\delta$  in these two figures was changed from kPa to Pa.

**Table 2. Descriptions of the asphalt binders.**

Name of Asphalt	Percent Polymer	PG of Base Asphalt	Description Provided by the Source	Trade Name	Source
<b>Unmodified Asphalts</b>	0	Not Applicable	PG 52-34, PG 64-28, PG 70-22	Not Applicable	Citgo Asphalt Refining Co.
<b>Air-Blown Asphalt</b>	0	52-34	Air-Blown Asphalt Without Catalyst	Not Applicable	Trumbull and Owens Corning
<b>Elvaloy</b>	2.2	50% 52-34 50% 64-28	Ethylene Terpolymer	Elvaloy	DuPont
<b>SBS Linear</b>	3.75	58.9% 52-34 41.1% 64-28	Styrene-Butadiene-Styrene	Dexco Vector 2518	TexPar Labs and Johns Manville
<b>SBS Linear Grafted</b>	3.75	58.9% 52-34 41.1% 64-28	Styrene-Butadiene-Styrene and 0.05% Additive	Dexco Vector 2518	TexPar Labs and Johns Manville
<b>SBS Radial Grafted</b>	3.25	58.9% 52-34 41.1% 64-28	Styrene-Butadiene-Styrene and 0.05% Additive	Shell 1184	TexPar Labs and Johns Manville
<b>EVA</b>	5.5	52-34	Ethylene Vinyl Acetate	Exxon Polybilt 152	TexPar Labs and Johns Manville
<b>EVA Grafted</b>	5.5	52-34	Ethylene Vinyl Acetate and 1.35% Additive	Exxon Polybilt 152	TexPar Labs and Johns Manville
<b>ESI</b>	5.0	52-34	Ethylene Styrene Interpolymer	ESI	Dow and PRI
<b>CMCRA</b>	5.0	64-28	Chemically Modified Crumb Rubber Asphalt	CMCRA	FHWA

**Table 3. Performance grade (PG) for each asphalt binder.**

Trade Name:	PG 52 Unmodified	PG 64 Unmodified	PG 70 Unmodified	Air-Blown Asphalt	Elvaloy	EVA	EVA Grafted
<b>PG:</b>	52-28	64-28	70-28	70-28	76-28	70-28	70-28
<b>Continuous PG:<sup>1</sup></b>	54-33	67-28	71-28	74-28	76-31	70-31	73-31
<b>PG From the Supplier:</b>	52-34	64-28	70-22	73-28	74-29	73-31	75-31
<b>Original Asphalt Binder</b>							
<b>Temperature at a <math>G^*/\sin\delta</math> of 1.00 kPa and 10 rad/s, C</b>	55	67	73	74	76	70	76
<b>RTFO Residue</b>							
<b>Temperature at a <math>G^*/\sin\delta</math> of 2.20 kPa and 10 rad/s, C</b>	54	67	71	74	77	75	74
<b>RTFO/PAV Residue</b>							
<b>Temperature at a <math>G^*\sin\delta</math> of 5000 kPa and 10 rad/s, C</b>	8.1	20	24	21	14	13	14
<b>BBR Temperature at a Creep Stiffness of 300 MPa and 60 s, C + 10°C</b>	-33	-28	-28	-29	-31	-31	-32
<b>BBR Temperature at an m-value of 0.30 and 60 s, C + 10°C</b>	-36	-30	-29	-28	-33	-31	-31
<b>Critical Cracking Temperature</b>	-35	-28	-27	-28	-34	-31	-33

e From the BBR and Direct Tension, C							
--------------------------------------	--	--	--	--	--	--	--

<sup>1</sup>The low-temperature continuous PG is the PG provided by the BBR.

**Table 3. Performance grade (PG) for each asphalt binder (continued).**

Trade Name:	SBS Linear	SBS Linear Grafted	SBS Radial Grafted	ESI	CMCRA
<b>PG:</b>	70-28	70-28	70-28	76-28	76-28
<b>Continuous PG:<sup>1</sup></b>	72-31	72-33	71-32	76-31	76-29
<b>PG from the Supplier:</b>	72-28	74-29	73-28	Unknown	76-28
<b>Original Asphalt Binder</b>					
<b>Temperature at a G*/sinδ of 1.00 kPa and 10 rad/s, C</b>	75	75	74	77	76
<b>RTFO Residue</b>					
<b>Temperature at a G*/sinδ of 2.20 kPa and 10 rad/s, C</b>	72	72	71	76	76
<b>RTFO/PAV Residue</b>					
<b>Temperature at a G*/sinδ of 5000 kPa and 10 rad/s, C</b>	18	15	16	9.2	18
<b>BBR Temperature at a Creep Stiffness of 300 MPa and 60 s, C + 10°C</b>	-32	-33	-32	-31	-29
<b>BBR Temperature at an m-value of 0.30 and 60 s, C + 10°C</b>	-31	-34	-32	-31	-29
<b>Critical Cracking Temperature From the BBR and Direct Tension, C</b>	-33	-34	-34	-29	-29

<sup>1</sup>The low-temperature continuous PG is the PG provided by the BBR.

**Table 4. Aggregate properties for the diabase.**

<b>Aggregate Gradations, Percent Passing:</b>					
<b>Sieve Size (mm)</b>	<b>61% No. 68 Diabase</b>	<b>30% No. 10 Diabase</b>	<b>8% Natural Sand</b>	<b>1% Hydrated Lime</b>	<b>Blend</b>
25.0	100.0				100.0
19.0	97.9				98.7
12.5	60.7				76.0
9.5	37.7	100.0	100.0		62.0
4.75	9.2	99.2	95.8		44.0
2.36	2.2	75.6	88.2		32.1
1.18	1.7	52.5	74.8		23.8
0.600	1.4	37.8	46.0		16.9
0.300	1.3	27.9	14.1		11.3
0.150	1.1	19.6	4.8		7.9
0.075	0.9	12.5	2.9	100.0	5.5
<b>Specific Gravities and Percent Absorption:</b>					
<b>Bulk Dry</b>	2.943	2.914	2.565		2.892
<b>Bulk SSD</b>	2.962	2.945	2.601		2.916
<b>Apparent</b>	2.999	3.007	2.659	2.262	2.961
<b>% Abs</b>	0.6	1.1	1.4		0.8
<b>Flat and Elongated Particles at a 3-to-1 Length-to-Thickness Ratio, Percent by Mass:</b>					
	21	NA	NA		
<b>Los Angeles Abrasion, Percent Loss by Mass:</b>					
	14	NA	NA		
<b>Fine Aggregate Angularity:</b>					
	NA	49	45		

Bulk Dry = Bulk Dry Specific Gravity  
 Bulk SSD = Bulk Saturated-Surface Dry Specific Gravity  
 Apparent = Apparent Specific Gravity  
 % Abs = Percent Water Absorption  
 NA = Not Applicable

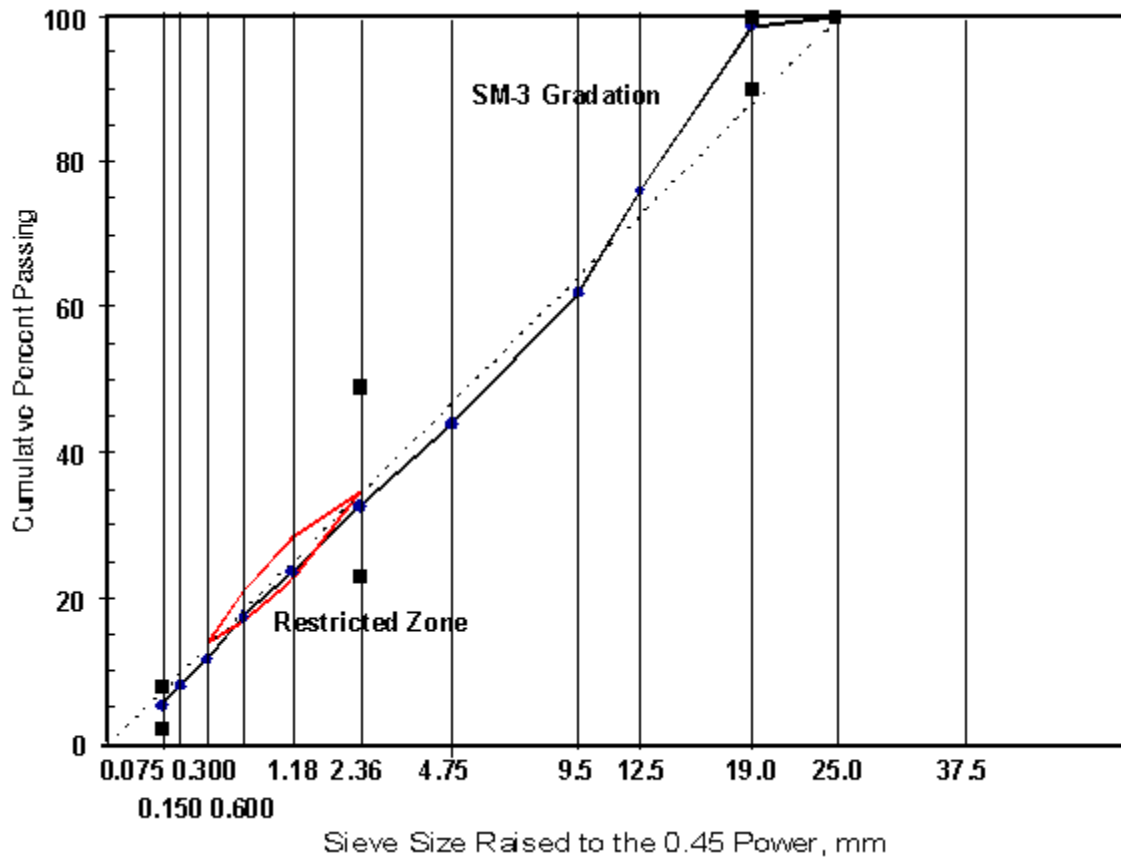


Figure 2. Aggregate gradation.

Table 5. Volumetric properties of the mixture.

Mixture Property	Diabase Mixture Without Hydrated Lime	Specification
<b>Asphalt Binder Content</b>		
Total Asphalt Binder Content, Percent by Mixture Mass	4.85	
Effective Asphalt Binder Content, Percent by Mixture Mass	4.15	
Asphalt Binder Absorption, Percent by Mixture Mass	0.7	
Effective Asphalt Binder Content, Percent by Total Volume	10.8	
<b>Voids Analyses</b>		
Maximum Specific Gravity of the Mixture	2.702	
Effective Specific Gravity of the Aggregate	2.948	
Total Air Voids, Percent by Volume	3.2	4.0
Voids in the Mineral Aggregate (VMA), Percent by Total Volume	14.0	Minimum of 13.0

Voids Filled With Asphalt (VFA), Percent by Total Volume	77	65 to 78
<b>Dust Content</b>		
Dust Content, Percent Finer Than 75 m by Aggregate Mass	5.5	
<b>Dust-to-Binder Ratios</b>		
Dust by Aggregate Mass to Total Binder Content by Mixture Mass	1.1	
Dust by Aggregate Mass to Effective Binder Content by Mixture Mass	1.3	0.6 to 1.6
Dust by Mixture Mass to Effective Binder Content by Mixture Mass	1.2	
Dust by Volume to Effective Binder Content by Volume	0.42	

Table 6.  $G^*/\sin\delta$ 's of all binders and mixtures with the materials listed from the highest to lowest mixture  $G^*/\sin\delta$ .

Asphalt Binder or Mixture Designation	Binder		Mixture	
	High Temp. PG	$G^*/\sin\delta$ , 50°C (kPa)	$G^*/\sin\delta$ , 50°C (MPa)	$G^*$ , 50°C (MPa)
	10.0 rad/s	10.0 rad/s	10.0 Hz	10.0 Hz
Novophalt (Validation Study)	77	60.2	101.5	84.5
Styrelf (Validation Study)	88	76.0	98.1	78.5
EVA Grafted	74	35.8	87.0	74.5
Air-Blown	74	49.1	85.8	75.8
PG 70-22	71	40.7	83.9	78.9
EVA	75	26.3	83.9	72.0
ESI	76	32.3	75.1	65.9
CMCRA	76	44.3	71.6	61.5
SBS Radial Grafted	71	25.1	55.1	50.1
AC-20 (Validation Study)	70	30.7	50.5	46.7
SBS Linear Grafted	72	25.6	47.8	43.9
SBS Linear	72	25.4	47.8	43.7
Elvaloy	77	28.7	46.4	39.7
PG 64-28	67	22.2	43.8	41.0
AC-10 (Validation Study)	65	15.9	29.1	26.9
AC-5 (Validation Study)	59	7.5	19.9	17.6
<b>Unmodified Asphalt Binders Only</b>				
PG 70-22	71	40.7	83.9	78.9
AC-20 (Validation Study)	70	30.7	50.5	46.7
PG 64-28	67	22.2	43.8	41.1
AC-10 (Validation Study)	65	15.9	29.1	26.9

AC-5 (Validation Study)	59	7.5	19.9	17.6
-------------------------	----	-----	------	------

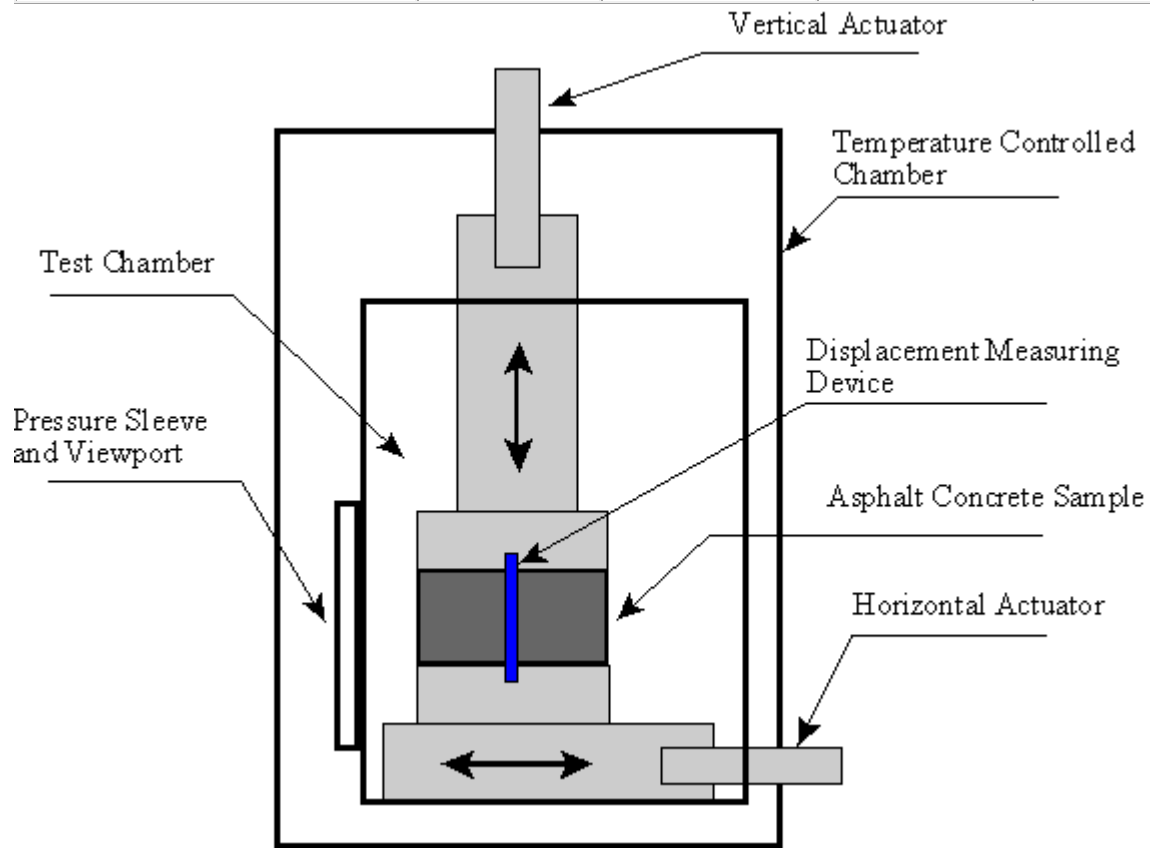


Figure 3. Diagram of SST chamber.



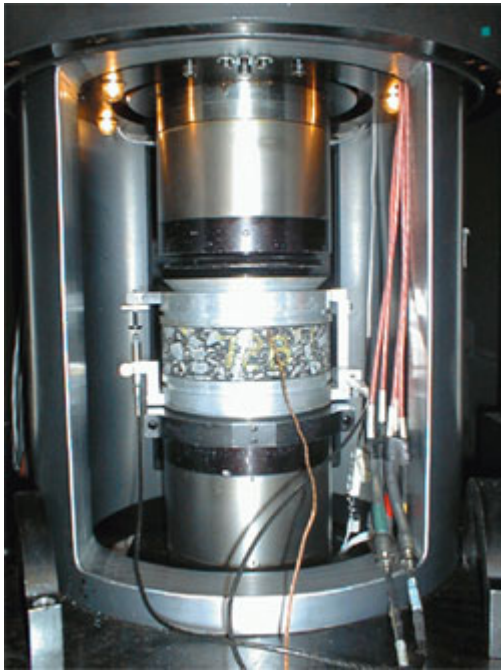


Figure 4. Superpave Shear Tester.

Table 7.  $G^*/\sin\delta$ 's of the 11 binders and mixtures with the materials listed from the highest to lowest mixture  $G^*/\sin\delta$ .

Asphalt Binder or Mixture Designation	Binder		Mixture				
	High Temp. PG	$G^*/\sin\delta$ 50°C (kPa)	$G^*/\sin\delta$ at 50°C (MPa)				
	10.0 rad/s	10.0 rad/s	10.0 Hz				
EVA Grafted	74	35.8	87.0	A			
Air-Blown	74	49.1	85.8	A			
PG 70-22	71	40.7	83.9	A			
EVA	75	26.3	83.9	A			
ESI	76	32.3	75.1	B			
CMCRA	76	44.3	71.6	B			
SBS Radial Grafted	71	25.1	55.1		C		
SBS Linear Grafted	72	25.6	47.8		C	D	
SBS Linear	72	25.4	47.8		C	D	
Elvaloy	77	28.7	46.4			D	
PG 64-28	67	22.2	43.8			D	
	10.0 rad/s	2.0 rad/s	2.0 Hz				
EVA Grafted	74	14.3	41.1	A			
EVA	75	12.1	39.3	A	B		
Air-Blown	74	14.2	38.6	A	B		

CMCRA	76	13.9	37.8	B				
ESI	76	8.9	34.5		C			
PG 70-22	71	10.2	29.9			D		
Elvaloy	77	10.0	25.5				E	
SBS Radial Grafted	71	7.6	24.9				E	F
SBS Linear Grafted	72	8.0	21.1					F
PG 64-28	67	5.4	20.5					G
SBS Linear	72	7.7	20.4					G

Table 8. Replicate data for  $G^*/\sin\delta$  at 50°C.

Asphalt Binder or Mixture Designation	Specimen No. 1	Specimen No. 2	Specimen No. 3	Average (MPa)	CV <sup>1</sup> (percent)
<b>Frequency = 10.0 Hz</b>					
EVA Grafted	85.5	91.3	84.3	87.0	4.3
Air-Blown	86.0	86.8	84.5	85.8	1.4
PG 70-22	94.0	69.9	87.8	83.9	14.9
EVA	79.5	84.3	87.8	83.9	5.0
ESI	80.3	71.1	73.8	75.1	6.3
CMCRA	68.1	76.9	69.7	71.6	6.5
SBS Radial Grafted	56.6	55.3	53.5	55.1	2.8
SBS Linear Grafted	41.8	51.4	50.3	47.8	11.0
SBS Linear	48.7	45.8	48.8	47.8	3.6
Elvaloy	45.0	46.1	48.1	46.4	3.4
PG 64-28	41.5	41.8	48.2	43.8	8.6
<b>Frequency = 2.0 Hz</b>					
EVA Grafted	41.1	42.7	39.4	41.1	4.0
EVA	38.1	39.2	40.7	39.3	3.3
Air-Blown	38.5	39.6	37.8	38.6	2.3
CMCRA	35.9	40.7	37.3	37.8	6.5
ESI	37.0	33.1	33.4	34.5	6.3
PG 70-22	28.1	27.6	34.1	29.9	12.1
Elvaloy	24.1	26.1	26.3	25.5	4.8
SBS Radial Grafted	25.2	25.5	24.1	24.9	3.0
SBS Linear Grafted	20.5	23.0	22.8	21.1	6.3
PG 64-28	20.9	19.5	21.0	20.5	4.1
SBS Linear	20.9	19.7	20.7	20.4	3.1

<sup>1</sup>CV = Coefficient of Variation, percent = (standard deviation ÷ average)\*100.

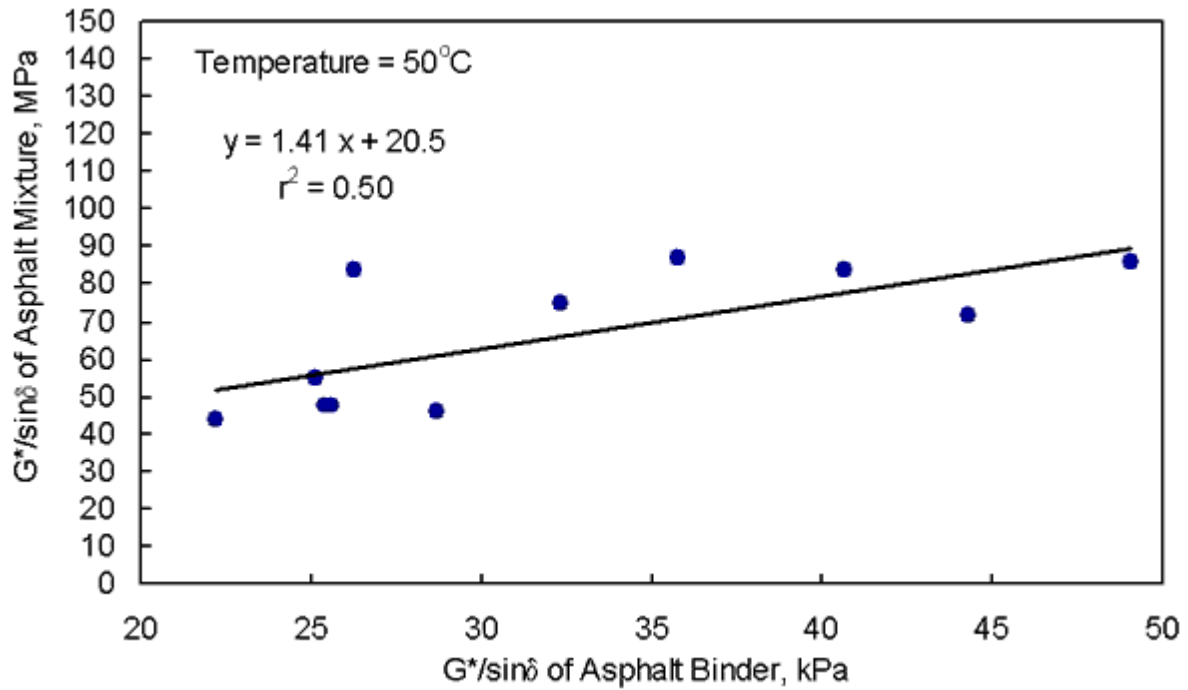


Figure 5.  $G^*/\sin\delta$  of the asphalt mixture vs.  $G^*/\sin\delta$  of the asphalt binder using the 11 asphalt binders.

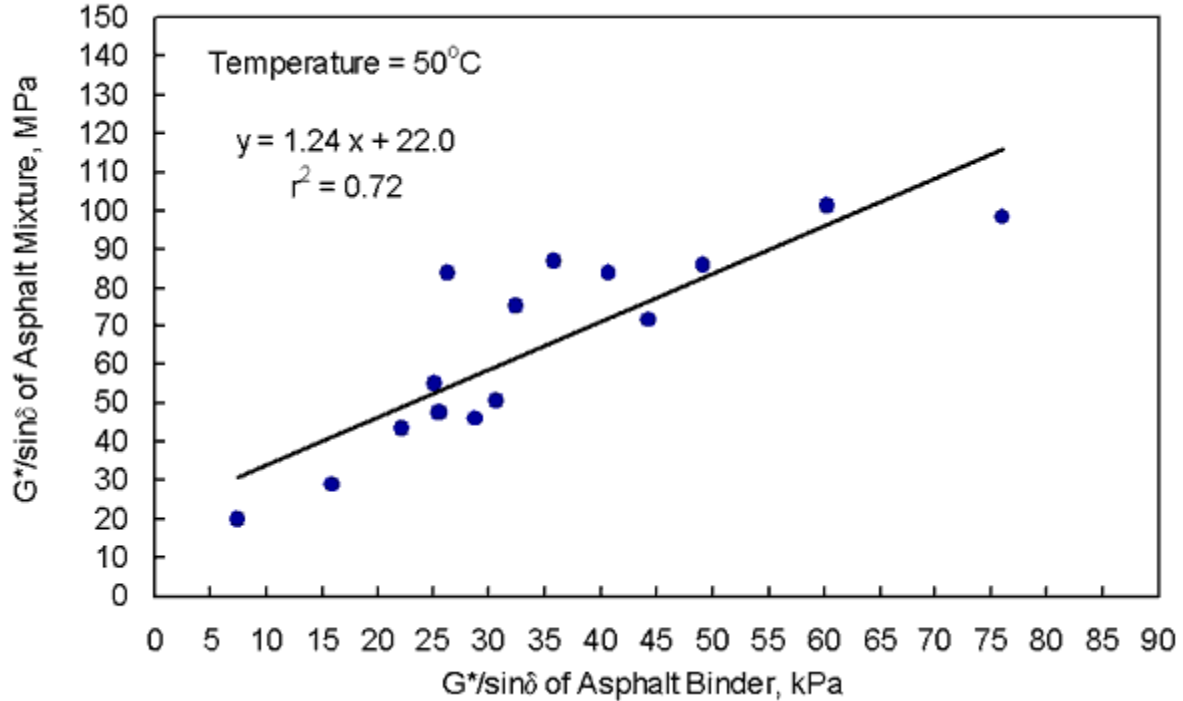


Figure 6.  $G^*/\sin\delta$  of the asphalt mixture vs.  $G^*/\sin\delta$  of the asphalt binder using all 16 asphalt binders.

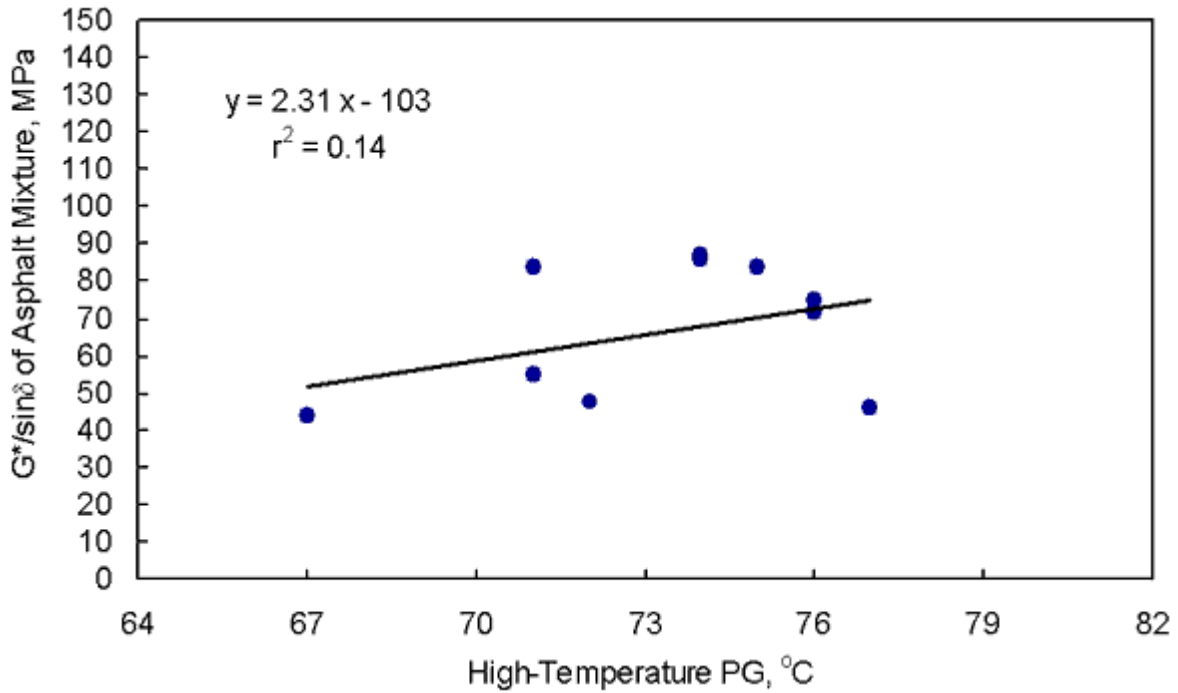


Figure 7.  $G^*/\sin\delta$  of the asphalt mixture at 50°C vs. high-temperature PG using the 11 asphalt binders.

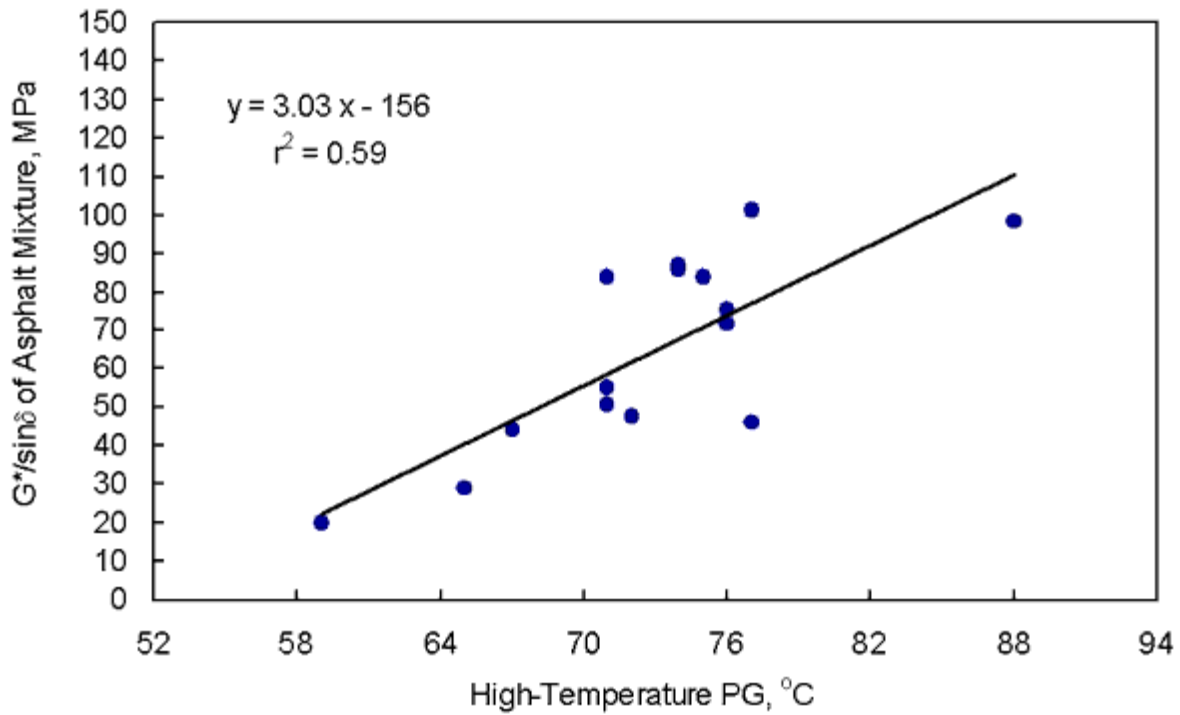


Figure 8.  $G^*/\sin\delta$  of the asphalt mixture at 50°C vs. high-temperature PG using all 16 asphalt binders.

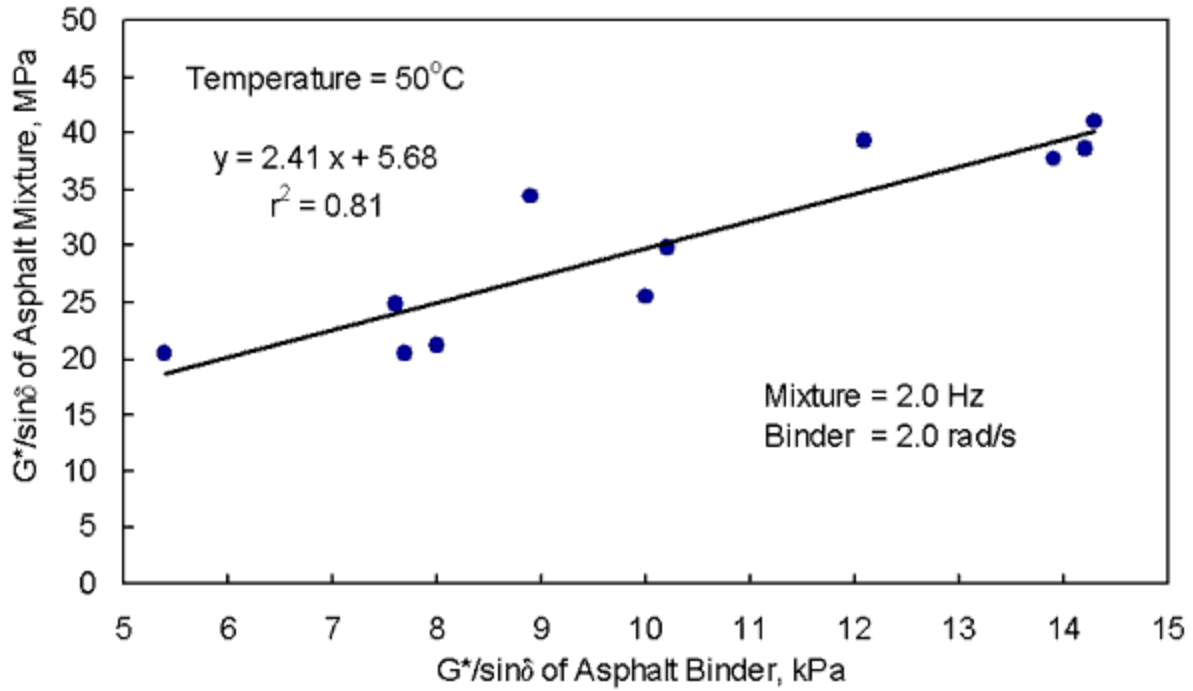


Figure 9.  $G^*/\sin\delta$  of the asphalt mixture at 2.0 Hz vs.  $G^*/\sin\delta$  of the asphalt binder at 2.0 rad/s using the 11 asphalt binders.

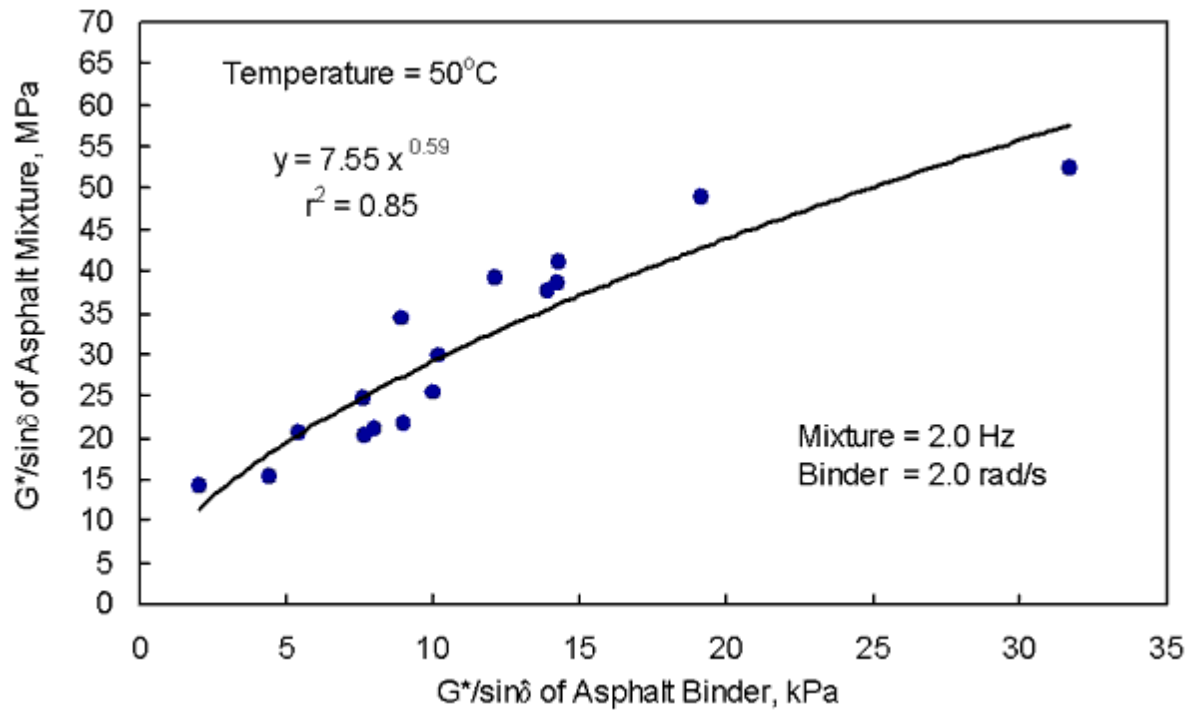


Figure 10.  $G^*/\sin\delta$  of the asphalt mixture at 2.0 Hz vs.  $G^*/\sin\delta$  of the asphalt binder at 2.0 rad/s using all 16 asphalt binders.

**Table 9.  $G^*/\sin\delta$ 's of the asphalt binders vs. cumulative permanent shear strain.**

Asphalt Binder or Mixture Designation	Binder		Mixture	Pavement
	High Temp. PG	$G^*/\sin\delta$ , 10.0 rad/s, 50°C (kPa)	Shear Strain, 50°C ( $\mu\text{m}/\text{m}$ )	Relative ALF Rut Depth (mm)
Styrelf (Validation Study)	88	76.0	10 500	6.1
EVA	75	26.3	13 600	7.3
Novophalt (Validation Study)	77	60.2	14 100	7.5
Elvaloy	77	28.7	14 600	7.7
EVA Grafted	74	35.8	15 400	8.0
CMCRA	76	44.3	19 100	9.7
SBS Radial Grafted	71	25.1	21 300	10.4
Air-Blown	74	49.1	21 300	10.4
ESI	76	32.3	22 700	11.0
SBS Linear Grafted	72	25.6	23 200	11.2
PG 70-22	71	40.7	23 900	11.4
SBS Linear	72	25.4	26 500	12.5
AC-20 (Validation Study)	70	30.7	36 200	16.4
PG 64-28	67	22.2	38 600	17.3
AC-10 (Validation Study)	65	15.9	61 300	26.4
AC-5 (Validation Study)	59	7.5	85 500	36.1
<b>Unmodified Asphalt Binders Only</b>				
PG 70-22	71	40.7	23 900	11.4
AC-20 (Validation Study)	70	30.7	36 200	16.4
PG 64-28	67	22.2	38 600	17.3
AC-10 (Validation Study)	65	15.9	61 300	26.4
AC-5 (Validation Study)	59	7.5	85 500	36.1

**Table 10. Statistical rankings for the 11 asphalt mixtures based on cumulative permanent shear strain.**

Asphalt Binder or Mixture Designation	Binder		Mixture						
	High Temp. PG	G*/sinδ, 10.0 rad/s, 50°C (kPa)	Cumulative Permanent Shear Strain, 50°C (μm/m)						
EVA	75	26.3	13 600	A					
Elvaloy	77	28.7	14 600	A					
EVA Grafted	74	35.8	15 400	A	B				
CMCRA	76	44.3	19 100	A	B	C			
SBS Radial Grafted	71	25.1	21 300		B	C	D		
Air-Blown	74	49.1	21 300		B	C	D		
ESI	76	32.3	22 700			C	D		
SBS Linear Grafted	72	25.6	23 200			C	D		
PG 70-22	71	40.7	23 900			C	D		
SBS Linear	72	25.4	26 500				D		
PG 64-28	67	22.2	38 600						E

**Table 11. Replicate data for the cumulative permanent shear strains.**

Asphalt Mixture	Cumulative Permanent Shear Strain at 50°C (μm/m)				CV <sup>1</sup> (percent)
	Specimen No. 1	Specimen No. 2	Specimen No. 3	Average	
EVA	15 100	12 900	12 800	13 600	9.6
Elvaloy	13 300	14 400	16 000	14 600	9.3
EVA Grafted	13 800	17 100	15 300	15 400	10.7
CMCRA	22 200	16 620	18 490	19 100	14.9
SBS Radial Grafted	16 200	21 400	26 300	21 300	23.7
Air-Blown	16 100	22 200	25 700	21 300	22.8
ESI	20 580	24 040	23 510	22 700	8.2
SBS Linear Grafted	21 500	18 600	29 400	23 200	24.1
PG 70-22	18 200	26 000	27 500	23 900	20.9
SBS Linear	29 500	23 400	26 700	26 500	11.5
PG 64-28	41 290	42 030	32 410	38 600	13.9

<sup>1</sup>CV = Coefficient of Variation, percent = (standard deviation ÷ average)\*100.

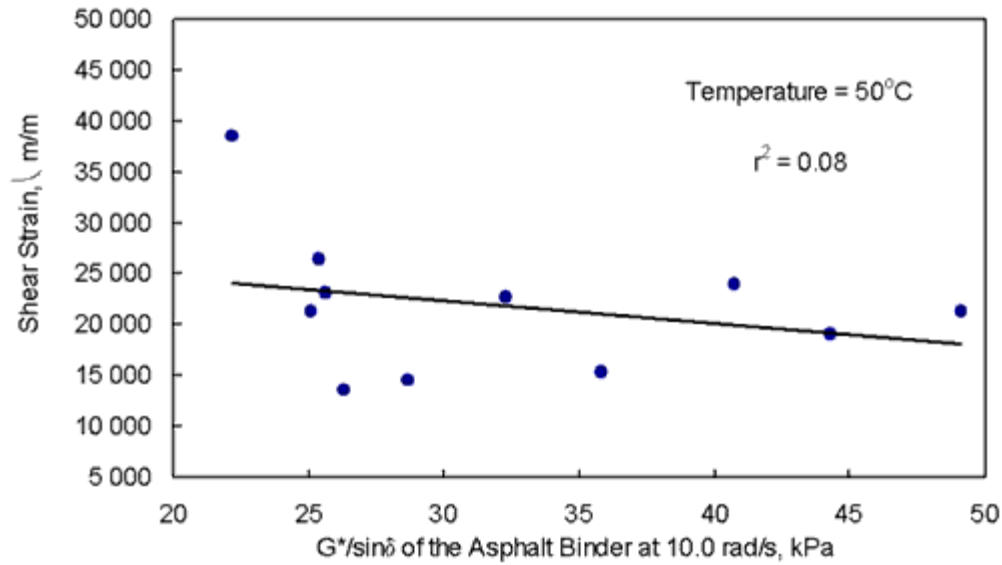


Figure 11. Cumulative permanent shear strain vs.  $G^*/\sin\delta$  of the asphalt binder at 10.0 rad/s using the 11 asphalt binders.

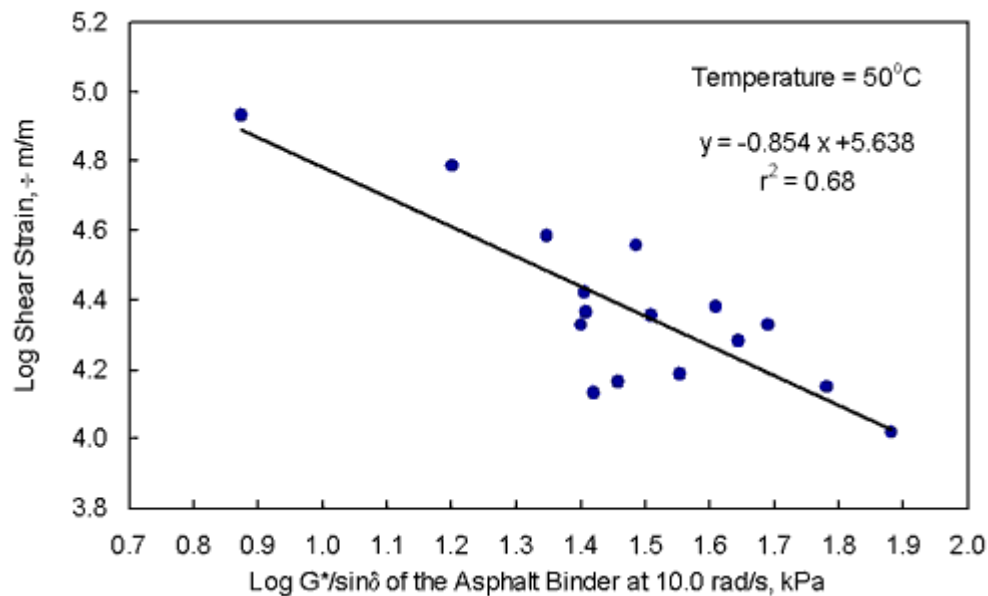
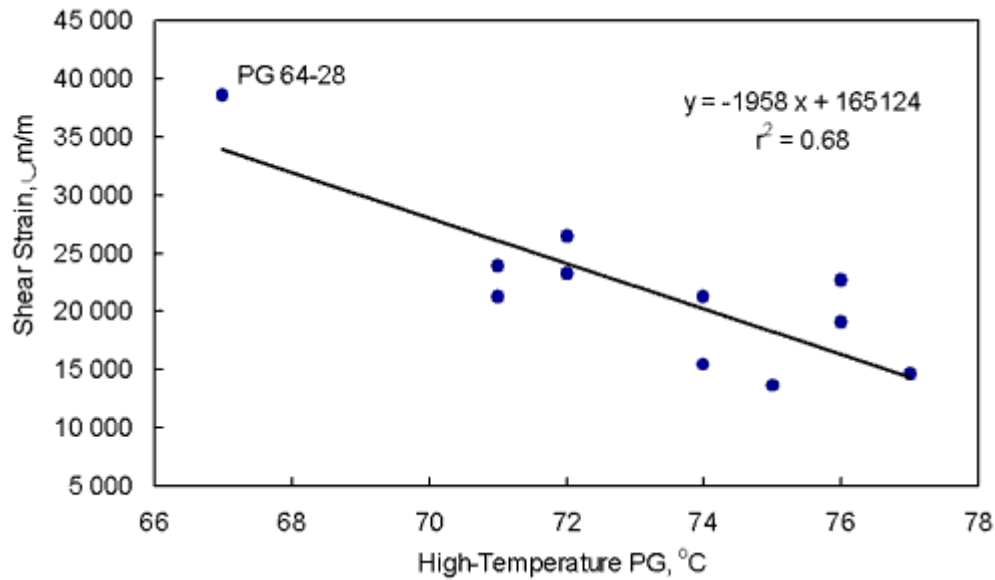
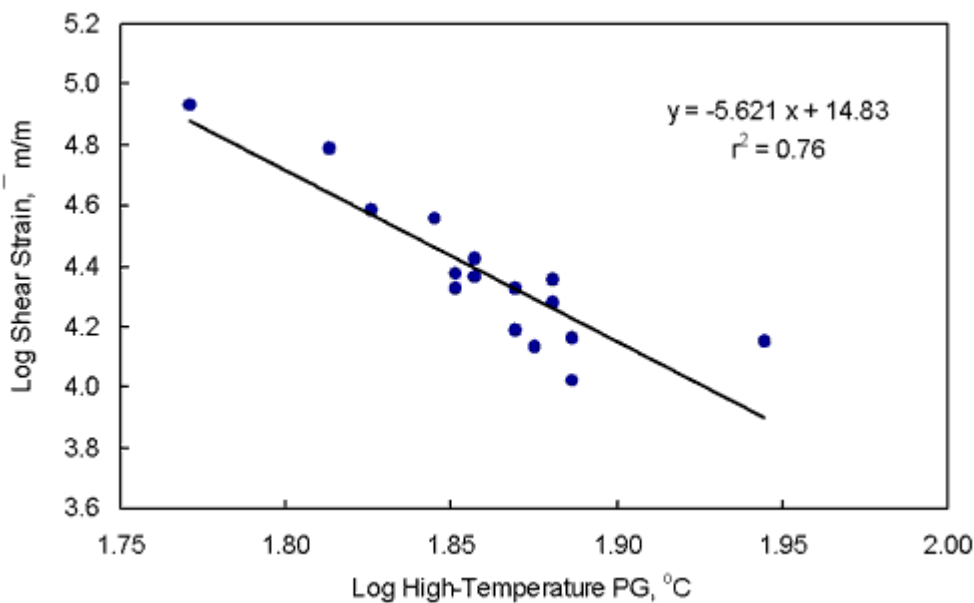


Figure 12. Log cumulative permanent shear strain vs. log  $G^*/\sin\delta$  of the asphalt binder at 10.0 rad/s using all 16 asphalt binders.





**Figure 13. Cumulative permanent shear strain at 50°C vs. high-temperature PG using the 11 asphalt binders.**



**Figure 14. Log cumulative permanent shear strain at 50°C vs. log high-temperature PG using all 16 asphalt binders.**

**Table 12.  $G^*/\sin\delta$ 's of the asphalt binders at 10.0, 2.0, and 0.125 rad/s with the asphalt binders listed from highest to lowest  $G^*/\sin\delta$  using 0.125 rad/s.**

Asphalt Binder	$G^*/\sin\delta$ at 50°C (kPa)		
	10.0 rad/s	2.0 rad/s	0.125 rad/s
Styrelf (Validation Study)	76.0	31.8	5.230
EVA	26.3	12.1	2.744
EVA Grafted	35.8	14.3	2.312
Novophalt (Validation Study)	60.2	19.1	2.000
Elvaloy	28.7	10.0	1.597
CMCRA	44.3	13.9	1.541
Air-Blown	49.1	14.2	1.390
SBS Linear Grafted	25.6	8.0	0.917
ESI	32.3	8.9	0.868
SBS Linear	25.4	7.7	0.811
PG 70-22	40.7	10.2	0.808
SBS Radial Grafted	25.1	7.6	0.802
AC-20 (Validation Study)	30.7	9.0	0.635
PG 64-28	22.2	5.4	0.405
AC-10 (Validation Study)	15.9	4.4	0.348
AC-5 (Validation Study)	7.5	2.1	0.130

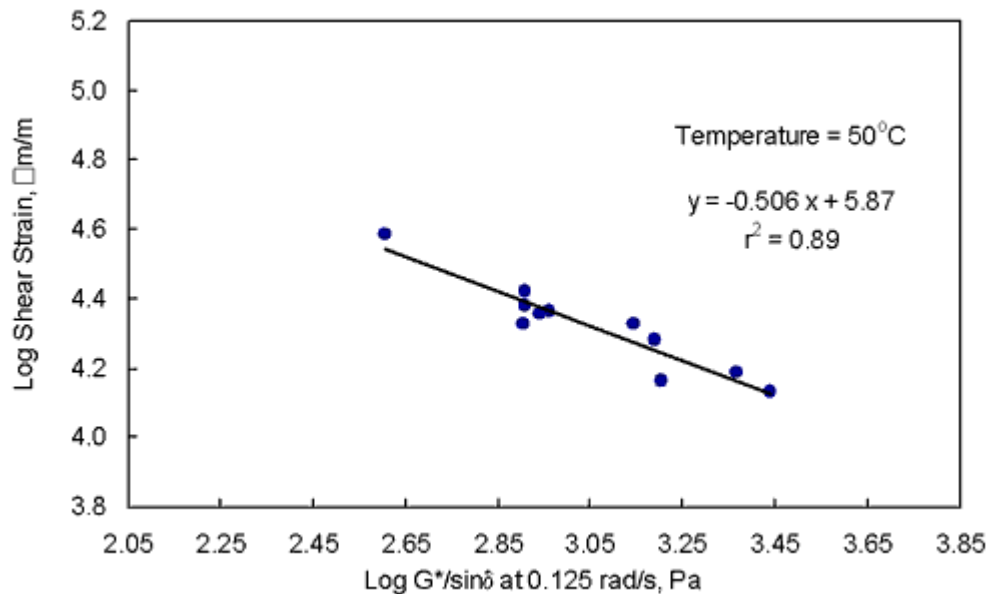


**Figure 15. Log cumulative permanent shear strain vs. log  $G^*/\sin\delta$  of the asphalt binder at 0.125 rad/s using the 11 asphalt binders.**

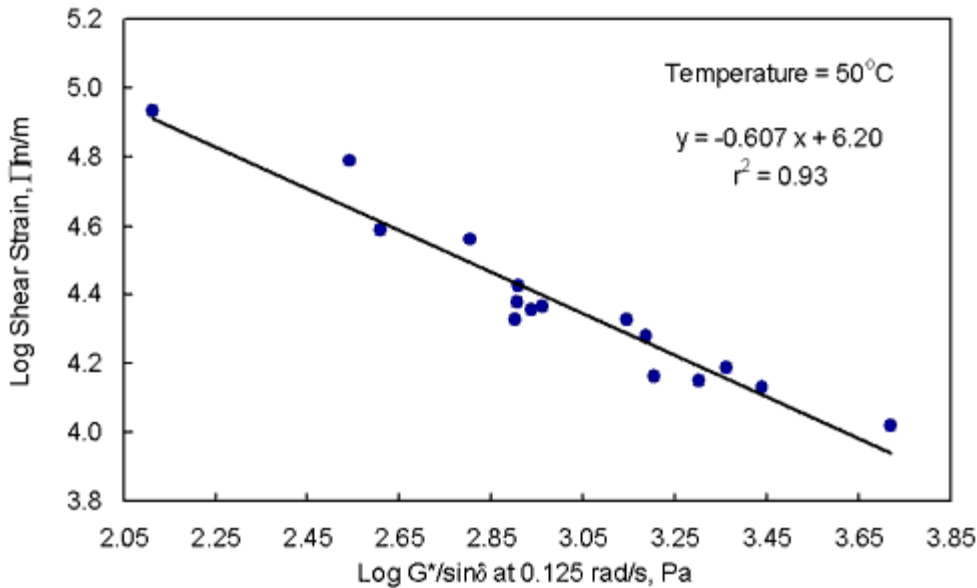


**Figure 16. Log cumulative permanent shear strain vs. log  $G^*/\sin\delta$  of the asphalt binder at 0.125 rad/s using all 16 asphalt binders.**

The following equation was provided by the five asphalt binders used in the Superpave Validation Study:

$$RD = 1.87 + 0.0004 (\text{CPSS}) \quad r^2 = 0.92 \quad (2)$$

where:

RD = Rut depth in the asphalt pavement layer at 58°C, mm.

CPSS = Cumulative permanent shear strain at 5,000 cycles and 50°C, µm/m.

The rut depths provided by equation 2 are included in table 9. Substituting the cumulative permanent shear strains of 28 750 to 18 100 µm/m into equation 2 provided rut depths of 13.4 and 9.1 mm, respectively. Therefore, an increase in PG from 70 to 76 provides a 32-percent reduction in rut depth. In the Superpave Validation Study, a change in strain from 28 750 to 18 100 µm/m would have provided a 50-percent reduction in rut depth. The applicability of equation 2 is questionable, but both studies indicate that an increase in PG from 70 to 76 should provide a significant decrease in the rate of pavement rutting for the particular mixture tested in this study.

In the Superpave Validation Study, Novophalt had the lowest cumulative permanent shear strain at 40°C at a 95-percent level of significance. Novophalt also had the highest resistance to pavement rutting at the three pavement test temperatures that were used: 58, 70, and 76°C. The data at 50°C in table 9 shows that Styrelf is ranked above Novophalt, although the strains for these two mixtures are not significantly different. Because the Novophalt mixture was more resistant to rutting according to both RSCH at 40°C and the pavement tests at 58, 70, and 76°C, it should have been more resistant to rutting when tested by RSCH at 50°C. This suggests that the change in ranking was the result of substituting diabase dust for hydrated lime. This change in ranking decreases the confidence in equation 2, even though the  $r^2$  of 0.92 is high.

## 7. French PRT

The French PRT tests a slab for permanent deformation using a smooth, rubber tire inflated to  $600 \pm 30$  kPa.<sup>(1)</sup> Each slab had a length of 500 mm, a width of 180 mm, and a thickness of 50 mm. The applied load was  $5000 \pm 50$  N and the test temperature was  $70^\circ\text{C}$ . The air-void level was 7.0 percent. The test normally ends at 6,000 wheel passes. In this study, the test was continued to 20,000 wheel passes to provide supplementary information. The French PRT is shown in figures 17 and 18.

Table 13 gives the rankings from Fisher's LSD for the average rut depths at 6,000 wheel passes. Only the mixture with the PG 64-28 asphalt binder had a significantly different average rut depth. The rut depths at 20,000 wheel passes provided the same ranking. The analysis indicated that the rut depths at 6,000 wheel passes need to differ by at least 2.1 mm for them to be different at a 5-percent level of significance.

The replicate data are given in table 14. Only one mixture, SBS Radial Grafted, had a high coefficient of variation. The coefficients are remarkably low for testing only two specimens per mixture.

For the 11 materials, figure 19 shows that the correlation between the rut depth at 6,000 wheel passes and  $G^*/\sin\delta$  at 0.9 rad/s was poor. The  $r^2$  was 0.52. A DSR frequency of 0.9 rad/s was used because it accounts for the slow speed of the French PRT.<sup>(1)</sup> The  $r^2$  increased from 0.52 to 0.70 using a log-log transformation, which indicates that there is a general trend of decreasing rut depth with increasing  $G^*/\sin\delta$ . The log-log relationship is shown in figure 20. Without EVA, the  $r^2$  would be 0.88.

Figure 21 shows that the correlation using the data from all asphalt binders and mixtures was poor. However, the relationship is curvilinear. Figure 22 shows the same data using a log-log transformation. The  $r^2$  increased from a poor value of 0.52 to a high value of 0.88. Without EVA, the  $r^2$  would be 0.93.

The high-temperature PG's provided fair to good correlations with the rut depths. Figure 23 shows that the  $r^2$  for the 11 asphalt binders and mixtures was 0.80. After excluding the data for the PG 64-28 materials, the  $r^2$  dropped to 0.71 and the range in the rut depths at 6,000 passes was only 6.5 to 8.5 mm.

Figure 24 shows that the  $r^2$  using all asphalt binders and mixtures was 0.80. The data for Styrelf was eliminated to determine if this would decrease the  $r^2$ . The  $r^2$  increased to 0.85. Based on the relationship given in figure 24, an increase of one high-temperature PG, from 70 to 76, would decrease the rut depth from 9.1 to 7.2 mm at  $70^\circ\text{C}$ , which is a 21-percent reduction. This is less than the 37-percent reduction provided by the cumulative permanent shear strains at  $50^\circ\text{C}$ . This may be due to the difference in test temperature or stress level. It is desirable that an increase of one PG be beneficial. However, a large difference in rutting performance would mean that the performances of asphalt binders within a grade could be significantly different. A decrease in rut depth of 20 to 40 percent with a change in PG seems reasonable.

In the Superpave Validation Study, Novophalt had the highest resistance to rutting according to the French PRT and ALF pavement tests.<sup>(1)</sup> The French PRT data in table 13 shows that Styrelf is ranked above Novophalt, although the rut depths for these two mixtures are not different at a 5-percent level of significance. No conclusion concerning the possible effect of hydrated lime could be made based on these results because both the test temperature and slab thickness were changed. A test temperature of  $60^\circ\text{C}$  and a slab thickness of 100 mm were used in the Superpave Validation Study, compared to  $70^\circ\text{C}$  and 50 mm in this study.

## 8. Hamburg WTD

The Hamburg WTD tests a slab of hot-mix asphalt submerged in hot water by rolling a steel wheel across its surface. The slabs tested in this study had a length of 320 mm, a width of 260 mm, and a thickness of 80 mm. Thicknesses up to 120 mm can be tested, and the thickness should be at least three times the nominal maximum aggregate size. The device tests two slabs simultaneously using two reciprocating solid steel wheels, each having a width of 47 mm. The applied load is 685 N and the average speed is 1.1 km/h. The rut depth in each slab is measured continuously over a length of 200 mm by a linear variable differential transformer. This rut depth does not include any upward heaving outside the wheelpath. After each user-specified increment of wheel passes is applied, the device stores the maximum rut depth along the 200-mm wheelpath relative to a rut depth of zero for the first wheel pass. It does not calculate an average rut depth. The standard maximum number of wheel passes is 20,000. This requires approximately 6.5 h. The pass/fail rut depth is 10 mm at 20,000 passes. Additional information on the Hamburg WTD is given elsewhere.<sup>(1,5-7)</sup> The device is shown in figure 25. The rut depths as a function of wheel passes are given in figure 26.

The creep slope from this device, which is the number of wheel passes needed to create a 1-mm rut depth, was used to evaluate the mixtures for their resistance to rutting. The creep slope is a measure of rutting resistance before moisture starts to significantly damage the specimen. Even so, some moisture damage may be included in the creep slope. Higher creep slopes indicate more resistance to rutting.

Two slabs were compacted per mixture at a  $7.0 \pm 0.5$ -percent air-void level. Each pair was tested at the same time. This meant that the test temperatures for the two slabs were identical, and each mixture was tested by both wheels, which accounts for any small differences in loading provided by them. The number of replicate specimens was insufficient for randomizing the tests.

The customary test temperature for the Hamburg WTD is 50°C, which was developed in Europe for a climate close to a Superpave high-temperature PG of 58. The test temperature used in this study was based on the amount of moisture damage provided by trial tests using the air-blown and unmodified PG 70-22 asphalt binders. The test temperature was not based on the creep slopes. Temperatures from 50 to 64°C were evaluated, and a temperature of 58°C seemed to be the optimum temperature for determining the effects of the asphalt binders on moisture resistance. This was based on both the rate of failure and the amount of visually stripped aggregate. Because water is used to control the test temperature, no slabs could be tested under dry conditions at 58°C. The effects of the asphalt binders on moisture sensitivity are reported elsewhere.<sup>(8)</sup>



**Figure 17. French Pavement Rutting Tester.**



**Figure 18. French PRT wheel and slab.**

**Table 13.  $G^*/\sin\delta$ 's of the asphalt binders vs. the French PRT with the materials listed from the lowest to highest rut depth at 6,000 wheel passes.**

Asphalt Binder or Mixture Designation	Binder		Mixture		
	High Temp. PG	$G^*/\sin\delta$ , 0.9 rad/s, 70°C (Pa)	Rut Depth at 70°C (mm)		
			2,000 Passes	6,000 Passes	20,000 Passes
Styrelf (Validation Study)	88	2360	3.6	4.8	6.2
Novophalt (Validation Study)	77	1020	5.0	6.0	7.2
Elvaloy	77	753	4.9	6.5 A	7.9
Air-Blown	74	439	5.4	6.8 A	9.0
CMCRA	76	566	5.4	6.8 A	9.7
EVA Grafted	74	394	5.7	7.5 A	10.4
ESI	76	500	5.5	7.6 A	9.2
EVA	75	203	6.0	7.6 A	10.1
SBS Linear Grafted	72	361	6.7	8.2 A	10.3
SBS Radial Grafted	71	312	6.7	8.2 A	10.4
PG 70-22	71	260	6.9	8.3 A	10.6
SBS Linear	72	309	7.0	8.5 A	10.5
AC-20 (Validation Study)	70	219	7.7	9.7	12.9
AC-10 (Validation Study)	65	118	8.8	10.7	15.1
PG 64-28	67	151	9.8	12.1 B	16.0
<b>Unmodified Asphalt Binders Only</b>					
PG 70-22	71	260	6.9	8.3	10.6
AC-20 (Validation Study)	70	219	7.7	9.7	12.9
AC-10 (Validation Study)	65	118	8.8	10.7	15.1
PG 64-28	67	151	9.8	12.1	16.0

Table 14. Replicate data for the French PRT.

Asphalt Mixture	Rut Depth at 6,000 wheel passes and 70°C (mm)			CV <sup>1</sup> (percent)
	Specimen No. 1	Specimen No. 2	Average	
Styrelf (Validation Study)	4.3	5.2	4.8	13.4
Novophalt (Validation Study)	6.0	5.9	6.0	12.9
Elvaloy	5.9	7.0	6.5	12.1
Air-Blown	6.4	7.1	6.8	7.3
CMCRA	6.6	6.9	6.8	3.1
EVA Grafted	7.0	8.1	7.5	10.3
ESI	8.3	6.8	7.6	14.0
EVA	6.8	8.5	7.6	15.7
SBS Linear Grafted	8.6	7.7	8.2	7.8
SBS Radial Grafted	6.5	9.9	8.2	29.3
PG 70-22	8.0	8.6	8.3	5.1
SBS Linear	8.6	8.4	8.5	1.7
AC-20 (Validation Study)	9.7	9.7	9.7	0.0
AC-10 (Validation Study)	10.6	10.8	10.7	1.3
PG 64-28	11.7	12.4	12.1	4.1

<sup>1</sup>CV = Coefficient of Variation, percent = (standard deviation ÷ average)\*100.

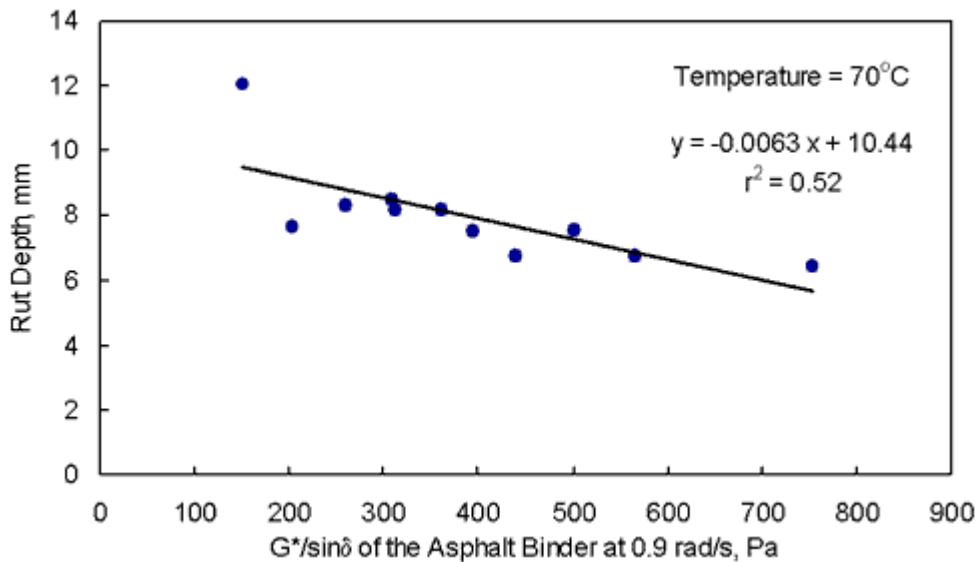


Figure 19. French PRT rut depth vs.  $G^*/\sin\delta$  of the asphalt binder at 0.9 rad/s using the 11 asphalt binders.



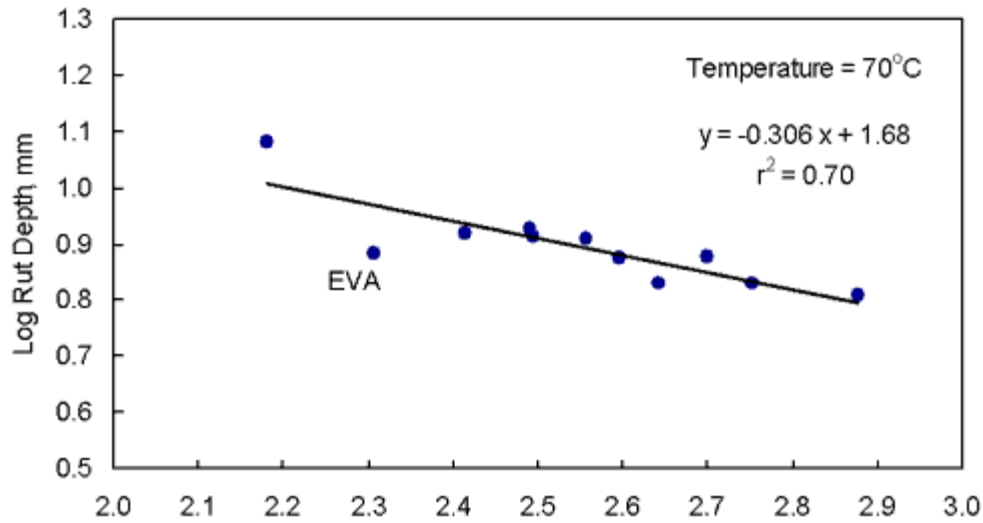


Figure 20. Log French PRT rut depth vs. log  $G^*/\sin\delta$  of the asphalt binder at 0.9 rad/s using the 11 asphalt binders.

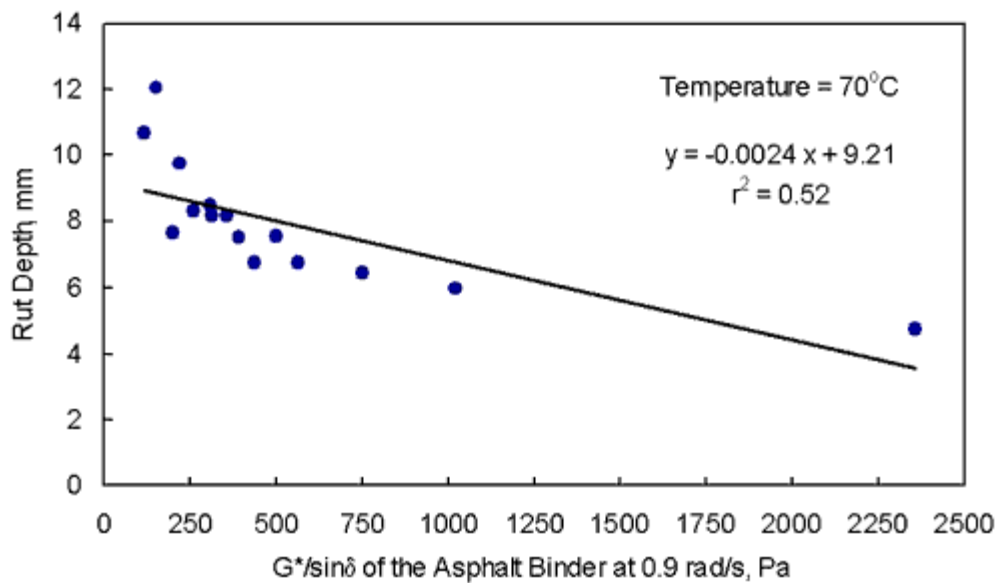


Figure 21. French PRT rut depth vs.  $G^*/\sin\delta$  of the asphalt binder at 0.9 rad/s using all asphalt binders.

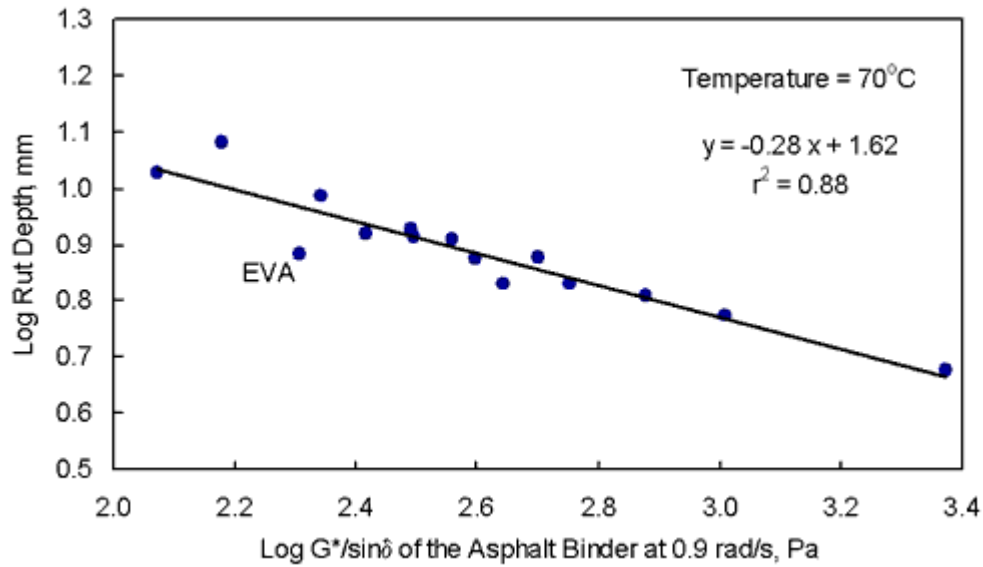


Figure 22. Log French PRT rut depth vs. log  $G^*/\sin\delta$  of the asphalt binder at 0.9 rad/s using all asphalt binders.

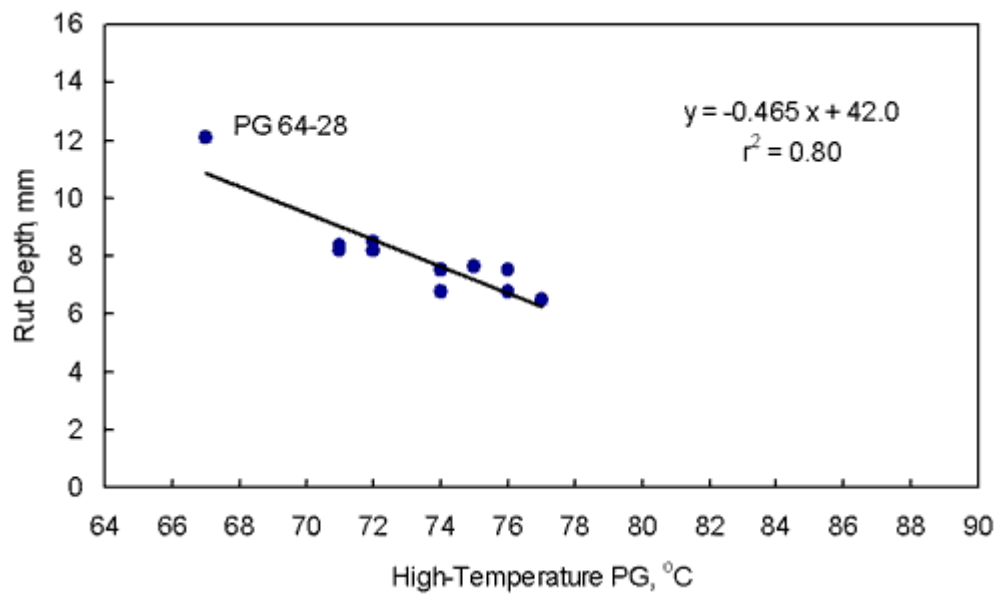
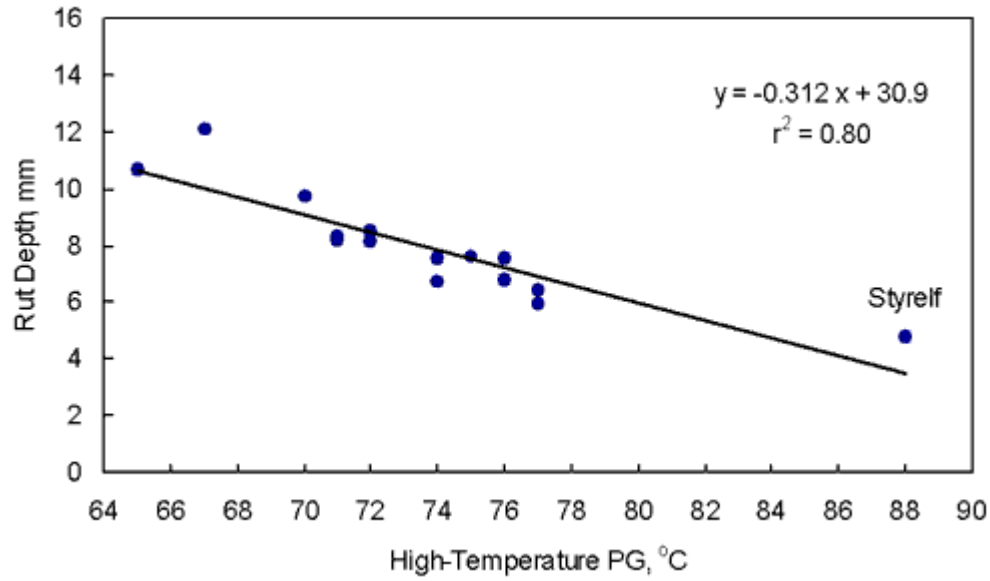


Figure 23. French PRT rut depth at 70°C vs. high-temperature PG using the 11 asphalt binders.



**Figure 24. French PRT rut depth at 70°C vs. high-temperature PG using all asphalt binders.**



**Figure 25. Hamburg Wheel-Tracking Device without water.**

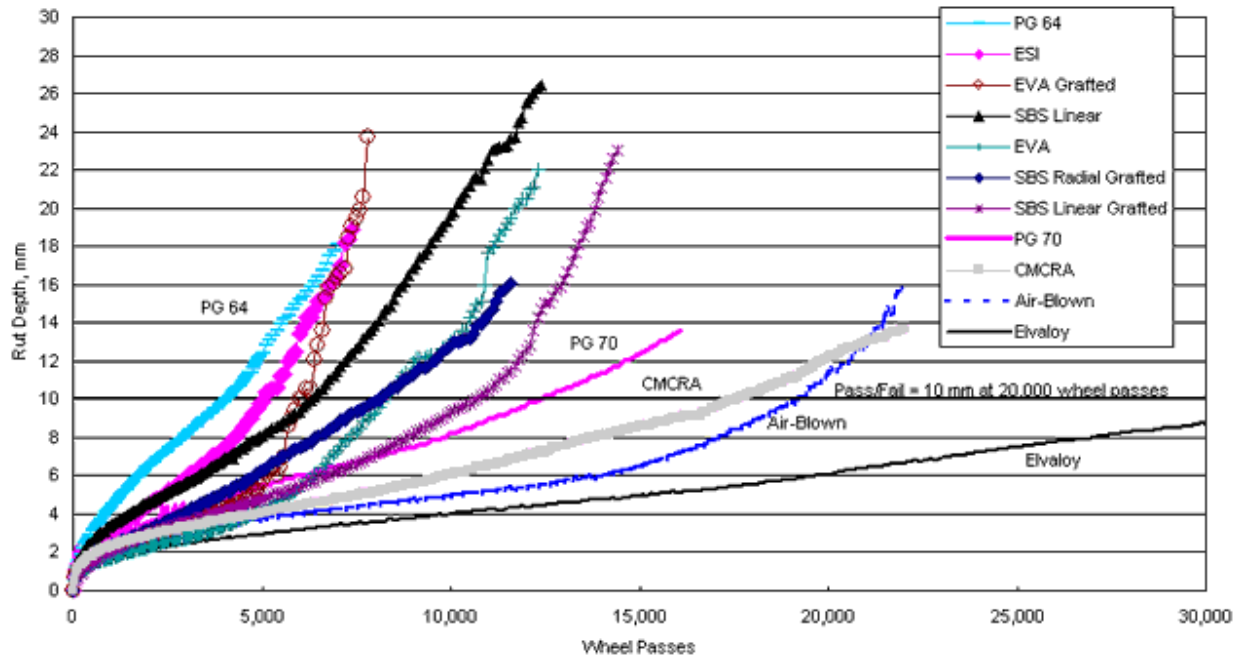


**Figure 26. Rut depth vs. wheel passes from the Hamburg WTD at 58°C.**

Table 15 provides the creep slopes. Three of the five asphalt binders used in the Superpave Validation Study were tested. The AC-5 and AC-10 asphalt binders were not tested because, in the former study, the mixtures with these binders failed rapidly. Both binders provided creep slopes at less than 700 passes/mm at 50°C, which was 8°C lower than the test temperature of 58°C used in this study.

Table 16 provides the replicate creep slopes. Many of the coefficients of variation are very poor, being above 30 percent. This is why 8 of the 11 mixtures fell into one group (group C) in table 15. The coefficients indicate that more slabs would have to be tested in order to have confidence in the averages.

The correlation between the creep slopes and  $G^*/\sin\delta$  at 0.125 rad/s for the 11 materials was poor. The  $r^2$  was 0.44. A frequency of 0.125 rad/s was used because it accounts for the slow speed of the Hamburg WTD.<sup>(1)</sup>  $G^*/\sin\delta$ 's at other DSR frequencies were also evaluated, but they did not provide higher  $r^2$ 's. There was no correlation between the creep slopes and high-temperature PG. The  $r^2$  was zero. This lack of a correlation could be expected based on the poor repeatability of the creep slopes.

The  $r^2$ 's from regression analyses using all 14 asphalt binders and mixtures were higher than for the 11 asphalt binders and mixtures. This was solely due to the inclusion of the data for Styrelf, which had the highest  $G^*/\sin\delta$  and creep slope. Without Styrelf, the  $r^2$ 's were poor.

## 9. Evaluation of Data Without Statistical Analysis

Table 17 provides rankings for the average cumulative permanent shear strains from RSCH and the average rut depths from the French PRT. These two tests were the primary tests used to evaluate rutting resistance. Rankings are also given for  $G^*/\sin\delta$  and the high-temperature PG's. The rankings in table 17 do not consider whether the differences in the averages are significant at a particular confidence level. Evaluating the rankings is also subjective.

Table 18 shows the results in terms of numerical rankings, where the ranking for each mixture test is considered the correct ranking. The rankings show that cumulative permanent shear strain correlates better with  $G^*/\sin\delta$  at 0.125 rad/s and 50°C than with high-temperature PG. The main discrepancy provided by  $G^*/\sin\delta$  at 0.125 rad/s is that the ranking for SBS Radial Grafted (No. 5) is low. However, SBS Radial Grafted is not an outlier based on the relationship shown in figure 15. All of the other numerical rankings for  $G^*/\sin\delta$  are not more than two positions away from where they should be based on the shear strains.

Table 18 shows that the main discrepancies provided by the French PRT are that the  $G^*/\sin\delta$  at 0.9 rad/s for EVA (No. 6) is low, and the high-temperature PG for the air-blown asphalt binder (No. 2) may be slightly low. The former discrepancy is supported by the relationship shown in figure 20, and also by figure 22. All of the other rankings are not more than two positions away from where they should be (based on the rut depths).

## 10. Comparison of Mixture Tests

Table 19 provides  $r^2$ 's from regression analyses performed on the data from the 11 mixtures. All of the  $r^2$ 's are poor except for the correlation between RSCH and the French PRT. The  $r^2$  is 0.75. This relationship is shown in figure 27. The  $r^2$  for the relationship without the PG 64-28 mixture is poor (0.40).

Table 20 provides  $r^2$ 's from regression analyses performed on the data from all mixtures. All of the  $r^2$ 's are poor, except for the correlations between RSCH and French PRT and between RSCH and FSCH using log-log transformations. The  $r^2$ 's are 0.76 and 0.73, respectively. The relationships are shown in figures 28 and 29, respectively. These relationships should not be used to predict one property from the other. The  $r^2$ 's are too low for prediction purposes. Table 20 shows that the next highest  $r^2$  was 0.69 between the French PRT and the Hamburg WTD.

## 11. Conclusions

### a. Conclusions Provided by the 11 Mixtures

The  $G^*/\sin\delta$ 's of the asphalt binders at 50°C and 0.125 rad/s had a high correlation to mixture rutting resistance as measured by the cumulative permanent shear strains from RSCH. The  $r^2$  was 0.89. (See figure 15.) The number of data points was insufficient for determining if there was a relationship between the continuous high-temperature PG and cumulative permanent shear strain.

The  $G^*/\sin\delta$ 's of the asphalt binders at 70°C and 0.9 rad/s had a weak correlation to mixture rutting resistance as measured by the French PRT at 70°C. The  $r^2$  was 0.70. (See figure 20.) Without EVA, the  $r^2$  would be 0.88. The continuous high-temperature PG's provided a fair correlation. The  $r^2$  was 0.80. (See figure 23.)

Grafting and the geometry of the EVA- and SBS-modified asphalt binders had no effect on their rutting resistances at a 5-percent level of significance.

The main objective of this study was to determine which asphalt binders provide high-temperature properties that do not agree with mixture rutting resistance. In general, the number of obvious discrepancies was low. The  $G^*/\sin\delta$  for EVA at 70°C and 0.9 rad/s was found to be low, based on the French PRT.

### b. Conclusions Provided by All Mixtures

The  $G^*/\sin\delta$ 's of the asphalt binders at 50°C and 0.125 rad/s had a high correlation to mixture rutting resistance as measured by the cumulative permanent shear strains from RSCH. The  $r^2$  was 0.93. (See figure 16.) The continuous high-temperature PG's provided a fair correlation. The  $r^2$  was 0.76. (See figure 14.)

The  $G^*/\sin\delta$ 's of the asphalt binders at 70°C and 0.9 rad/s had a high correlation to mixture rutting resistance as measured by the French PRT at 70°C. The  $r^2$  was 0.88. (See figure 22.) Without EVA, the  $r^2$  would be 0.93. The continuous high-temperature PG's provided a fair correlation. The  $r^2$  was 0.80. (See figure 24.)

The best correlations between the mixture tests were: (1) RSCH vs. French PRT,  $r^2 = 0.76$ ; (2) RSCH vs. FSCH,  $r^2 = 0.73$ ; and (3) French PRT vs. Hamburg WTD,  $r^2 = 0.69$ . These relationships should not be used to predict one property from the other. The  $r^2$ 's are too low for prediction purposes.

The creep slopes from the Hamburg WTD had very low repeatability.

A change in high-temperature PG from 70 to 76 significantly increased rutting resistance based on both RSCH and the French PRT. The reduction in cumulative permanent shear strain from RSCH at 50°C was 37 percent. The reduction in rut depth from the French PRT at 70°C was 21 percent. Based on these reductions, it could be concluded that there can be differences in rutting performance for asphalt binders within a grade, but this conclusion has to be balanced against the increase in the number of grades if the increment between grades was to be reduced.

## 12. Recommendations

The correlations between mixture  $G^*/\sin\delta$  and binder  $G^*/\sin\delta$  were fair to good. The  $r^2$  for the 16 materials was 0.79 using 10.0 Hz and 10.0 rad/s, and 0.85 using 2.0 Hz and 2.0 rad/s. There is no fundamental reason for choosing these pairs of frequencies, and they do not relate mathematically to each other. Therefore, the data could be correlated using a matrix of several asphalt mixture frequencies vs. several asphalt binder frequencies.

The asphalt binders should be tested using other aggregate types or gradations, and, if possible, the test temperature for the SST should be increased so that it is closer to the PG's of the asphalt binders.

Determine whether the elimination of the hydrated lime from the mixture caused the change in ranking for the Novophalt and Styrelf mixtures and the changes in the moduli shown in table 1.

## 13. References

1. K. D. Stuart, W. S. Mogawer, and P. Romero, *Validation of Asphalt Binder and Mixture Tests That Measure Rutting Susceptibility Using the Accelerated Loading Facility*, Publication No. FHWA-RD-99-204, Federal Highway Administration, McLean, VA, December 1999, 348 pp.
2. *AASHTO Provisional Standards*, American Association of State Highway and Transportation Officials, Washington, D.C., April 2000 Edition.
3. NCHRP Project 90-07, "Understanding the Performance of Modified Asphalt Binders in Mixtures," Work Plan, Study in Progress, National Cooperative Highway Research Program (NCHRP), Transportation Research Board, National Research Council, Washington, D.C., 2001.

4. AASHTO TP5, "Method for Determining the Rheological Properties of Asphalt Binder Using a Dynamic Shear Rheometer," *AASHTO Provisional Standards*, American Association of State Highway and Transportation Officials, Washington, D.C., April 2000 Edition.
5. T. Aschenbrener, "Evaluation of the Hamburg Wheel-Tracking Device to Predict Moisture Damage in Hot-Mix Asphalt," *Transportation Research Record 1492*, Transportation Research Board, Washington, D.C., 1995, pp. 193-201.
6. T. Aschenbrener, R. Terrel, and R. Zamora, *Comparison of the Hamburg Wheel-Tracking Device and the Environmental Conditioning System to Pavements of Known Stripping Performance*, Publication No. CDOT-DTD-R-94-1, Colorado Department of Transportation, Denver, CO, January 1994.
7. M. Hines, "The Hamburg Wheel-Tracking Device," *Proceedings of the Twenty-Eighth Paving and Transportation Conference*, Civil Engineering Department, The University of New Mexico, Albuquerque, NM, 1991.
8. K.D. Stuart, J.S. Youtcheff, and W.S. Mogawer, "*Understanding the Performances of Modified Asphalt Binders in Mixtures: Evaluation of Moisture Sensitivity*," Publication No. FHWA-RD-02-029, Federal Highway Administration, McLean, VA, December 2001, 17 pp.

**Table 15.  $G^*/\sin\delta$ 's of the binders vs. the creep slopes from the Hamburg WTD with the materials listed from highest to lowest slope (highest to lowest resistance to rutting).**

Asphalt Binder or Mixture Designation	Binder		Mixture			
	High Temp. PG	$G^*/\sin\delta$ , 0.125 rad/s, 58°C (Pa)	Creep Slope, 58°C (passes/mm)			
<b>Styrelf (Validation Study)</b>	88	2480	7000			
<b>Elvaloy</b>	77	639	4900	A		
<b>CMCRA</b>	76	482	3200	A		
<b>Air-Blown</b>	74	387	3900	A	B	
<b>PG 70-22</b>	71	213	2200		B	C
<b>Novophalt (Validation Study)</b>	77	651	2040			
<b>EVA</b>	75	751	2000			C
<b>SBS Linear Grafted</b>	72	297	1300			C
<b>EVA Grafted</b>	74	727	1300			C
<b>SBS Radial Grafted</b>	71	249	1100			C
<b>AC-20 (Validation Study)</b>	70	226	1000			
<b>SBS Linear</b>	72	248	900			C
<b>ESI</b>	76	321	790			C
<b>PG 64-28</b>	67	114	500			C

**Table 16. Replicate data for the Hamburg WTD.**

Asphalt Mixture	Creep Slope (passes/mm)			CV <sup>1</sup> (percent)
	Specimen No. 1	Specimen No. 2	Average	
<b>Elvaloy</b>	4650	5070	4900	6.1
<b>Air-Blown</b>	4340	3510	3900	15.0
<b>CMCRA</b>	5970	1330	3650	89.9
<b>CMCRA (Repeat)</b>	3770	1555	2700	58.8
<b>PG 70-22</b>	1000	3390	2200	80.0
<b>EVA</b>	2770	1200	2000	55.9
<b>SBS Linear Grafted</b>	1560	1090	1300	25.1
<b>EVA Grafted</b>	1080	1430	1300	19.7
<b>SBS Radial Grafted</b>	610	1600	1100	63.4
<b>SBS Linear</b>	690	1130	900	34.2
<b>ESI</b>	690	930	800	21.0
<b>PG 64-28</b>	450	550	500	14.1

<sup>1</sup>CV = Coefficient of Variation, percent = (standard deviation ÷ average)\*100.

**Table 17. Rankings by test type with the material having the most resistance to rutting listed at the top.**

SST			French PRT		
Mixture	Binder		Mixture	Binder	
Cumulative Permanent Shear Strain, 50°C	G*/sinδ, 0.125 rad/s, 50°C	High Temp. Continuous PG	Rut Depth, 70°C	G*/sinδ, 0.9 rad/s, 70°C	High Temp. Continuous PG
EVA	EVA	Elvaloy	Elvaloy	Elvaloy	Elvaloy
Elvaloy	EVA Grafted	CMCRA	Air-Blown	CMCRA	CMCRA
EVA Grafted	Elvaloy	ESI	CMCRA	ESI	ESI
CMCRA	CMCRA	EVA	EVA Grafted	Air-Blown	EVA
SBS Radial Grafted	Air-Blown	Air-Blown	ESI	EVA Grafted	Air-Blown
Air-Blown	SBS Linear Grafted	EVA Grafted	EVA	SBS Linear Grafted	EVA Grafted
ESI	ESI	SBS Linear Grafted	SBS Linear Grafted	SBS Radial Grafted	SBS Linear Grafted
SBS Linear Grafted	SBS Linear	SBS Linear	SBS Radial Grafted	SBS Linear	SBS Linear
PG 70-22	PG 70-22	PG 70-22	PG 70-22	PG 70-22	PG 70-22
SBS Linear	SBS Radial Grafted	SBS Radial Grafted	SBS Linear	EVA	SBS Radial Grafted



**Table 18. Numerical rankings by test type where No. 1 has the most resistance to rutting according to the test and No. 11 has the least resistance to rutting.**

SST RSCH			French PRT		
Mixture	Binder		Mixture	Binder	
Cumulative Permanent Shear Strain, 50°C	G*/sinδ, 0.125 rad/s, 50°C	Continuous High Temp. PG	Rut Depth, 70°C	G*/sinδ, 0.9 rad/s, 70°C	Continuous High Temp. PG
1	1	2	1	1	1
2	3	4	2	3	3
3	2	7	3	5	5
4	4	1	4	2	6
5	6	6	5	4	2
6	8	3	6	7	4
7	7	8	7	8	7
8	10	10	8	10	10
9	9	9	9	9	9
10	5	5	10	6	8
11	11	11	11	11	11

**Table 19. Coefficients of determination, r<sup>2</sup>, using the data from the 11 mixtures.**

	SST FSCH G*/sinδ, 10.0 Hz, 50°C	French PRT Rut Depth, 70°C	Hamburg WTD Creep Slope, 58°C
SST RSCH Shear Strain, 50°C	0.14 Log-Log: 0.12	0.75 Log-Log: 0.59	0.20 Log-Log: 0.36
SST FSCH G*/sinδ, 10.0 Hz, 50°C		0.10 Log-Log: 0.11	0.00 Log-Log: 0.01
French PRT Rut Depth, 70°C			0.38 Log-Log: 0.62

**Table 20. Coefficients of determination,  $r^2$ , using the data from all mixtures.**

	SST FSCH $G^*/\sin\delta$ , 10.0 Hz, 50°C	French PRT Rut Depth, 70°C	Hamburg WTD Creep Slope, 58°C
SST RSCH Shear Strain, 50°C	0.56 Log-Log: 0.73	0.66 Log-Log: 0.76	0.33 Log-Log: 0.51
SST FSCH $G^*/\sin\delta$ , 10.0 Hz, 50°C		0.48 Log-Log: 0.47	0.09 Log-Log: 0.17
French PRT Rut Depth, 70°C			0.51 Log-Log: 0.69

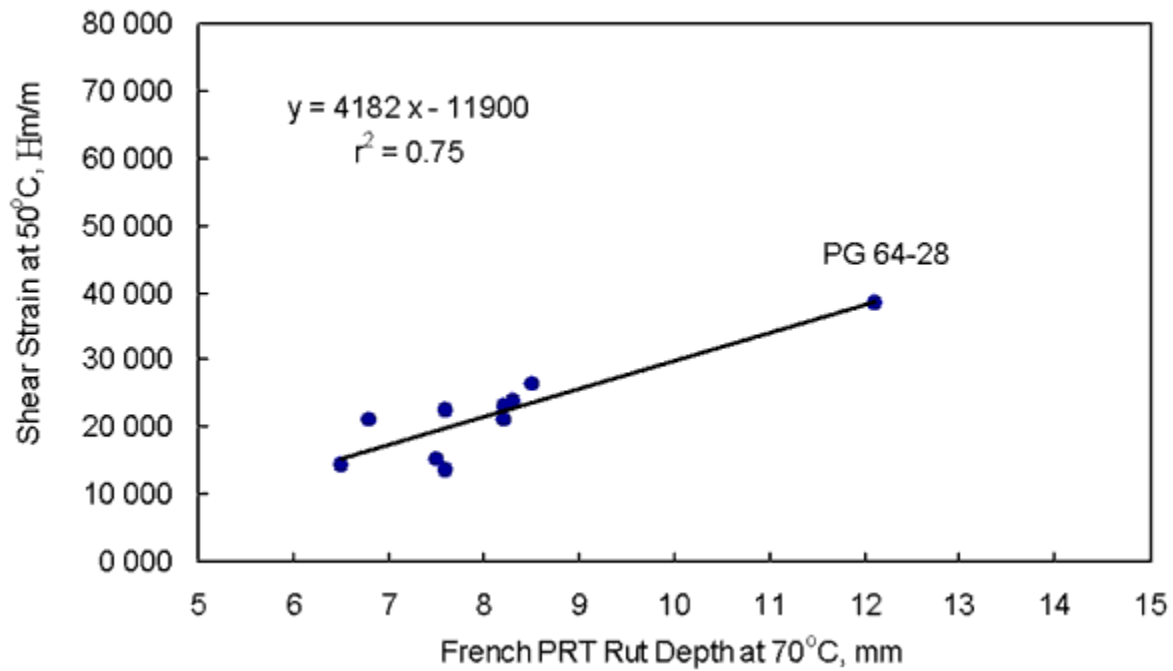


**Figure 27. RSCH cumulative permanent shear strain at 50°C vs. French PRT rut depth at 70°C for the 11 mixtures.**

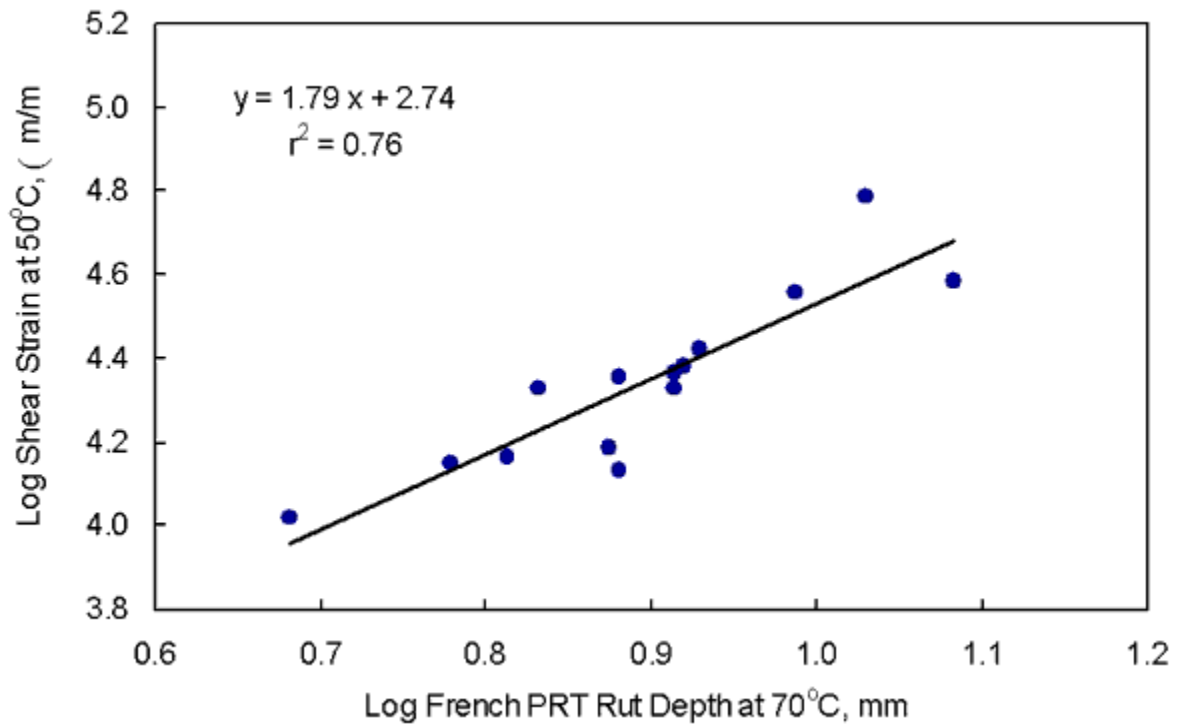
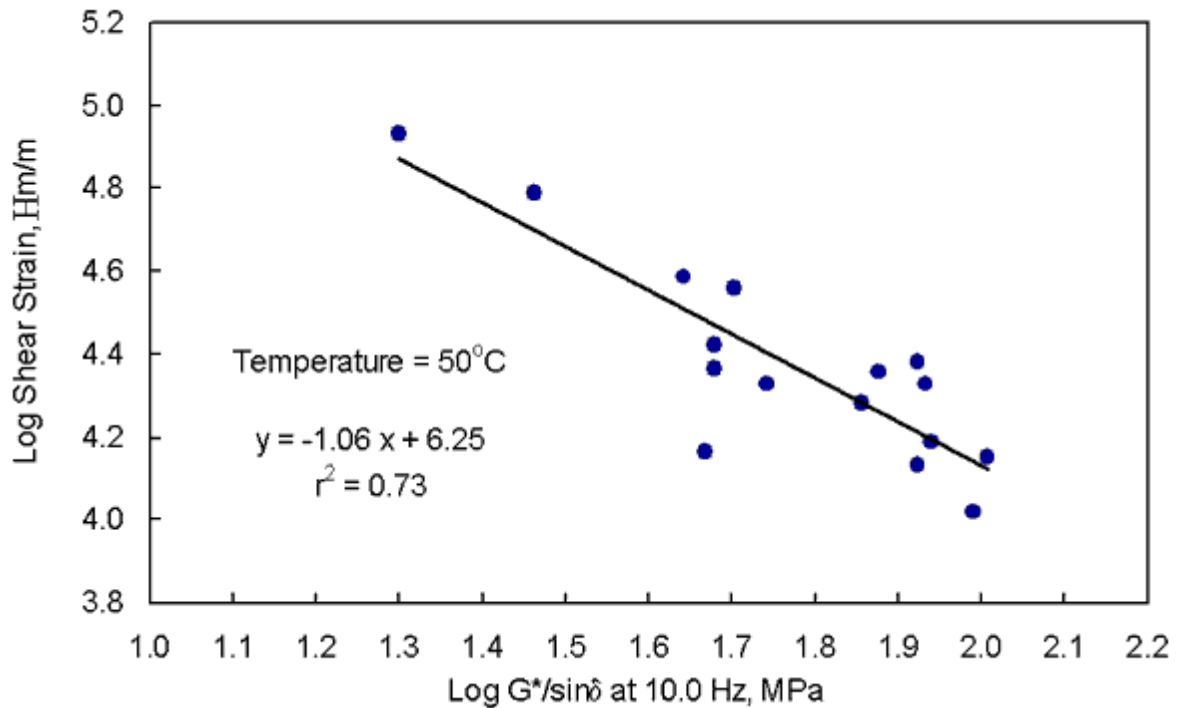


Figure 28. Log RSCH cumulative permanent shear strain at 50°C vs. log French PRT rut depth at 70°C for all mixtures.



**Figure 29. Log RSCH cumulative permanent shear strain vs. log FSCH  $G^*/\sin\delta$  for all mixtures.**

## PERSONNEL

John S. Youtcheff and Kevin D. Stuart, FHWA, Turner-Fairbank Highway Research Center, 6300 Georgetown Pike, McLean, VA 22101-2296

Walaa S. Mogawer, Civil and Environmental Engineering Department, University of Massachusetts Dartmouth, North Dartmouth, MA 02747

Naga Shashidhar, Susan Needham, Scott Parobeck, and Frank Davis, SaLUT, Turner-Fairbank Highway Research Center, 6300 Georgetown Pike, McLean, VA 22101-2296

Aroon Shenoy, Senior Research Fellow, FHWA, Turner-Fairbank Highway Research Center, 6300 Georgetown Pike, McLean, VA 22101-2296